ORNL/TM-2022/2373

Biofuel Viability for the Ocean-Going Marine Sector

Mike Kass[1]
Eric Tan[2]
Karthikeyan K. Ramasamy[4]
Troy Hawkins[3]
Tim Theiss[1]
Zia Abdullah[2]
Meltem Urgun-Demirtas[3]
Asanga Padmaperuma[4]
Corinne Drennan[4]
Joshua Schaidle[4]
Emily Newes[2]
Kristi Moriarty[2]
Doug Longman[3]
Kristiina Iisa[2]
Calvin Mukarakate[2]
Brian Kaul[1]
Shuyun Li[4]
Suh-Jane Lee[4]
Mond Gui[2]
Michael Thorson[2]
George G. Zaimes[3]
Jaxon Z. Stuhr[3]

[1]Oak Ridge National Laboratory
[2]National Renewable Energy Laboratory
[3]Argonne National Laboratory
[4]Pacific Northwest National Laboratory

March 2022

OAK RIDGE National Laboratory

U.S. DEPARTMENT OF ENERGY

ORNL IS MANAGED BY UT-BATTELLE LLC FOR THE US DEPARTMENT OF ENERGY

ORNL/TM-2022/2373

Buildings and Transportation Science Division

BIOFUEL VIABILITY FOR THE OCEAN-GOING MARINE SECTOR

Mike Kass[1]
Eric C. D. Tan[2]
Karthikeyan K. Ramasamy[4]
Troy Hawkins[3]
Tim Theiss[1]
Zia Abdullah[2]
Meltem Urgun-Demirtas[3]
Asanga Padmaperuma[4]
Corinne Drennan[4]
Joshua Schaidle[3]
Emily Newes[2]
Kristi Moriarty[2]
Doug Longman[3]
Kristiina Iisa[2]
Calvin Mukarakate[3]
Brian Kaul[1]
Shuyun Li[4]
Suh-Jane Lee[4]
Mond Gui[4]
Michael Thorson[4]
George G. Zaimes[3]
Jaxon Z. Stuhr[3]

[1]Oak Ridge National Laboratory
[2]National Renewable Energy Laboratory
[3]Argonne National Laboratory
[4]Pacific Northwest National Laboratory

March 2022

Prepared by
OAK RIDGE NATIONAL LABORATORY
Oak Ridge, TN 37831-6283
managed by
UT-BATTELLE LLC
for the
US DEPARTMENT OF ENERGY
under contract DE-AC05-00OR22725

CONTENTS

LIST OF FIGURES

LIST OF TABLES

ABSTRACT

Marine transport contributes significantly to global carbon dioxide emissions but is one of the most difficult sectors to decarbonize because full electrification is infeasible. Renewable, low–carbon biofuels offer a potential path to decarbonization of the marine sectors but the understanding of the effects of new biofuels on engine performance and emissions is limited. In this document we report on the results of a series of studies on the techno-economic, life cycle and technical feasibility of biofuels as replacements for heavy fuel oils currently used to fuel large ocean-going vessels.

1. INTRODUCTION

Before the 1950s, marine cargo vessels were powered using diesel fuel. However, the cheapest fuel available was the residual fraction of crude oil. Therefore, the industry began to move away from more expensive and highly processed distillate fuels in favor of heavy residual fuel oil (HFO). These fuels primarily comprise the residual fractions of crude, and therefore contain high levels of contaminants, including water, sulfur, and ash (solids). These contaminants must be removed before burning in an engine. Additionally, residual fuels have high viscosity because of their composition of high–molecular weight (MW) hydrocarbons. Therefore, these fuels must be heated to reduce their viscosity and improve their flow properties. HFO is stored around 50°C in onboard storage tanks and is further heated to 90°C (or higher) during purification and delivery to the engine. Despite the energy (and hence cost) penalties associated with impurity removal and viscosity reduction, burning HFO rather than distillate fuels is more economical for ship owners for most ocean-going applications. Currently, approximately 60% of all ocean-going vessels are fueled using HFO, which includes the large cargo and container vessels used to transport more than 80% of international goods. The total amount of HFO consumed for maritime use is estimated to be around 300 MMT per year, which corresponds to approximately 6% of the total annual oil demand (Kass et al. 2018). Consequently, maritime HFO use contributes significantly to anthropogenic greenhouse gas (GHG) emissions. It is estimated that the marine shipping sector accounts for 2% to 3% of the global CO_2 emissions. Black carbon emissions from shipping, which totaled approximately 67 kt in 2015, also have a significant environmental impact (Comer, et al. 2017).

The International Maritime Organization (IMO) is a specialized agency within the United Nations responsible for developing the regulatory framework and standards for the shipping industry. It purview includes ship design, construction, equipment, manning, operation, and disposal. In 2020, the IMO set new regulations that set the maximum allowable sulfur content of 0.5% w/w for marine heavy fuel oil, when a scrubber is not employed. The IMO has also introduced new policies focused on GHG reduction. In 2013, the IMO introduced the Energy Efficiency Design Index (IMO, 2019), providing a regulatory framework and metric for reducing emissions of CO_2 per metric ton–mile from shipping by approximately 10% per decade (IMO 2019). More recently, the IMO adopted a resolution targeting a 50% reduction in GHGs by 2050, relative to a 2008 baseline (IMO 2018); the IMO also plans to develop marine black carbon regulations in the coming years. This level of GHG reduction will not be possible through efficiency increases alone, as shown in Figure 1. GHG emissions from global shipping are also among the most difficult to eliminate (Davis, et al. 2018), and the marine market will continue to rely on liquid fuels rather than electrification for the foreseeable future. Thus, new low-carbon fuels are needed to reduce CO_2 emissions from global shipping. This effort would constitute a large new potential market for both electrofuels and biofuels.

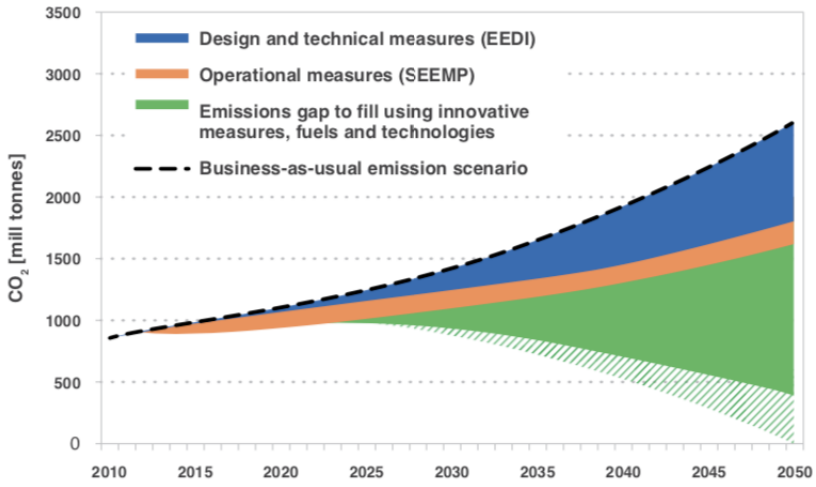

Figure 1. Marine CO_2 emissions outlook.

Approximately two-thirds of global marine fuel consumption is in large ocean-going cargo vessels propelled by low-speed two-stroke diesel engines (Concawe 2017), as shown in Figure 2. These engines are primarily operated on HFO/very low sulfur fuel oil (VLSFO) and are highly efficient and tolerant of viscous, low-quality fuels.

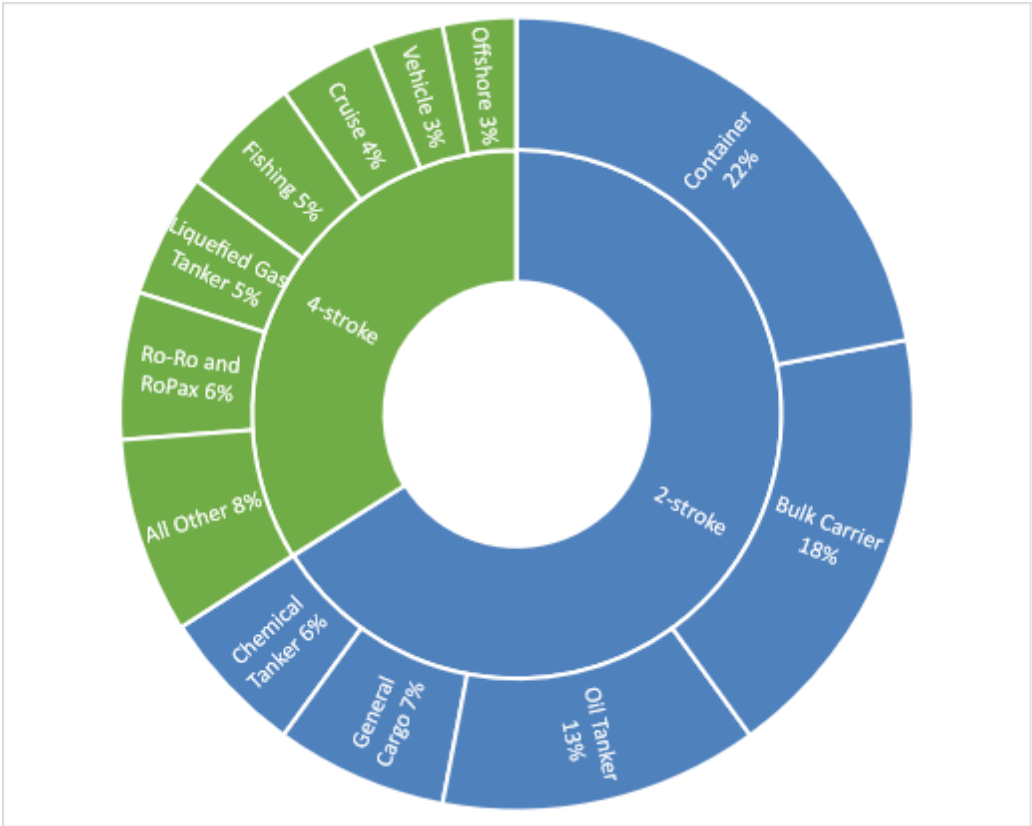

Figure 2. Fuel consumption by ship main engine type. Data from Concawe (2017).

As previously stated, HFOs require significant on-board conditioning and treatment systems to remove catalyst fines and other abrasive contaminants, heat the fuel to allow for pumping/handling, and further

control the temperature to achieve a target viscosity for fuel injection. Bunkering these fuels is also nontrivial because mixing of incompatible batches of fuel may lead to precipitation of asphaltenes, which causes significant operational and cleanup challenges, including plugged filters and the formation of large solid masses that must be manually chipped out of fuel tanks. Onboard and laboratory testing of fuels is conducted prior to operation, and ship systems are tuned to the properties of the fuel that was bunkered.

The objective of this project is to provide the foundational information and demonstrations that will lead to a FOA-based ship engine demonstration of an advanced biofuel for FY2025. For FY22 this effort seeks to determine the minimal upgrading of bio-intermediates for use with heavy fuel oils. This effort addresses BETO goals of developing and advancing bioenergy production technologies and establish the use of biofuels as a sustainable and cleaner marine fuel. The research team has set up an external advisory board (EAB) comprised of shipowners, fuel suppliers, and industry representatives to provide guidance and input. This board is critical to exchanging information between the research team and the industry, especially on identifying industry concerns, interests, and research needs. This effort also seeks input and guidance from a marine shipowner, or engine manufacturer, to assist in the research strategy towards what will be acceptable for use in a ship.

A key motivation for this effort centered on the applicability of biofuels derived from pyrolysis and hydrothermal liquefaction (HTL) conversion processes. These processes can utilize almost any biomass source, including waste sludge and woody feedstocks; if the biomass sources are used in the raw state, they are inexpensive to produce relative to other biofuel types, such as biodiesel, bio-alcohols, and renewable diesel. Mature biofuels, such as diesel, ethanol, and renewable diesel, were analyzed, and diesel that was made by the Fischer–Tropsch (FT) process was examined. These biofuels served as baselines along with HFO and marine distillates. Institutions, such as Maersk and GoodFuels, are also investigating biofuels as a replacement or substitute for HFO. Their studies have focused on economics and emissions benefits. The present study is unique in that it draws upon experimental data. There is a huge lack of experimental data for biofuels for marine applications because of the lack of availability of large two-stroke crosshead engines for research purposes. Therefore, studies have been primarily limited to four-stroke engines, which operate under conventional diesel compression ignition combustion. A couple of industry standards can be employed, including the ASTM 4740 spot test and the estimated cetane number test. The ASTM 4749 spot test is used to determine the compatibility or blend stability of HFOs. The chemistry of HFOs can vary considerably and when one heavy oil is added (i.e., blended) with another, there is a potential that the asphaltene component of HFOs will precipitate. Asphaltenes are unique to HFOs; they contain polar aliphatic side groups and can readily precipitate if the chemistry changes, which can happen during bunkering when mixing fuels.

The chemistry and composition of residual fuel oils are distinguished from distillate fuels in that they contain a highly colloidal dispersion of high-MW polymers that have complex structures. These polymers are known as asphaltenes, and they exist in chemical equilibrium with the surrounding fuel oil (Concawe 2017, Jun et al. 2013, Hofko et al. 2016, Rogel et al. 2001). The asphaltenes along with saturates, aromatics, and resins make up the primary components of HFOs and are categorized by their solubility and absorption properties [Garaniya et al. 2011, McKay et al. 1978). Asphaltenes have large polyaromatic carbon-fused ring structures that contain small paraffinic side chains, as shown in Figure 3. The outer side structures are primarily functional groups of carboxylic acids, carbonyls, phenols, and potentially pyrroles and pyridines (Gawrys and Kilpatrick 2004). These side groups are capable of dipole–dipole and hydrogen bonding interactions with the surrounding fluid, which—along with the dispersion forces of the aromatic rings—are responsible for determining whether asphaltenes remain suspended in the residual fuel oil. The continuous phase surrounding the asphaltenes comprises saturates, aromatics, and resins. In the complex mixture of residual fuel oil, the asphaltene and surrounding liquid phase remain as a colloidal dispersion as long as the solubility forces (i.e., dispersion, polarity, and hydrogen bonding) between the asphaltene and surrounding fluid are similar. The relatively high polarity of the asphaltene requires that

the surrounding fluid must have similar polarity to maintain a stable suspension. The addition of nonpolar solvents to residual fuel oils has been demonstrated to lower the solubility of asphaltenes, causing them to fall out of solution as a precipitate (McKay et al. 1978). The propensity of asphaltenes to precipitate determines fuel and blend stability. Asphaltene precipitation is the primary cause of filter plugging, fouling, and flow difficulties of residual fuel oils (McKay et al. 1978). Therefore, stability tests are typically performed on residual fuels prior to bunkering aboard a vessel.

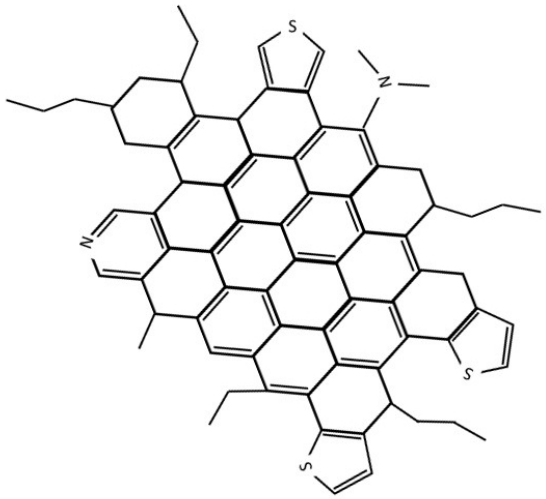

Figure 3. Diagram of an asphaltene molecule showing primary ring structures and aliphatic side chains.

In 2018, the US Department of Energy (DOE) Bioenergy Technologies Office sponsored a study involving Oak Ridge National Laboratory (ORNL), Argonne National Laboratory (ANL), Pacific Northwest National Laboratory (PNNL), and the National Renewable Energy Laboratory (NREL) to explore whether opportunities existed for biofuels in the marine sector, especially as low-sulfur fuels for large ocean-going vessels. The results of this study were published and provided a favorable initial assessment and highlighted the existing research needs (Kass et al. 2018). This report examined, at a cursory level, the potential benefits, feasibility, and barriers to the use of biofuels in place of heavy fuel oil (HFO) and marine gas oil for marine vessels. It led to a larger effort in which preliminary techno-economic analysis (TEA) and life cycle analysis (LCA) were conducted along with key technical feasibility efforts, which are discussed in this report.

2. SUPPLY AND DEMAND CURVE STUDIES AND TEA FOR BASELINE FUELS AND BIOFUELS

The TEA combines process modeling with experimental results (or actual operating data) to provide an economic evaluation. Thus, it provides guidance on the economic viability of a process and provides directions to research and development. This section also includes analysis of port supply and demand curve analysis.

2.1 DATA SOURCES AND APPROACH FOR ASSESSING BASELINE FUEL OIL COSTS

For the economic analyses, obtaining the representative data was difficult because of the limited sources. Detailed data sets were only available from the ports of Panama, Seattle–Tacoma, and Singapore. Only these ports provided sufficient useful data for supply and demand curve studies and TEA. The International Energy Agency's (IEA's) World Energy Statistics (OECD, 2020) provided information pertaining to bunker fuel oil consumption, which was used in these analyses. This information provided fuel consumption use for vessels engaged in international navigation (excluding ships used for military and fishing purposes).

The navigational activity of international shipping was assessed using the total container throughput from UNCTAD (2020). This throughput, or cargo capacity, is expressed in units of 20 ft equivalents, which is based on the volume of a 20 ft long container used in transporting goods. Fuel oil prices were determined using the annual average price of marine fuel oils (380 CST and 180 CST grades) for the Port of Singapore (Argus 2021). Brent Crude was also used in pricing assessments since it is the most highly traded HFO type. The pricing of Brent Crude was obtained from data provided by the International Monetary Fund (IMO 2021). The monthly bunkering fuel sales (in metric tons) and activity (in thousand 20 ft equivalents) were based on data supplied for each port studied (Autoridad Maritima de Panama, 2021; Maritime and Port Authority of Singapore, 2021; State of Washington, 2021; the Northwest Seaport Alliance, 2021).

The pricing results for each port are the average monthly price of 380 CST marine fuel oil (except for Singapore, which is the average monthly price of both 380 cSt and 180 cSt) from Argus (2021). These results are shown Figure 4. As shown in the figure, the average price of fuel oil depends on port location at any given time. Recent data shows that the price is relatively constant for the ports studied (~$350/ton).

A two-stage least squares econometrics analysis was conducted to determine if crude oil prices are a reliable indicator for bunker fuel price, which was found to be the case. At the global level, port activity showed a significant and positive effect on fuel demand (port activity increases with fuel demand), as expected.

However, the price elasticity of fuel (i.e., the change in demand resulting from a change in cost) was not significant. (A possible explanation for this finding might be a measurement error regarding global bunker fuel sales.) As noted by the US Environmental Protection Agency (EPA) (2008), global data on marine fuel demand varies considerably across sources. Marine fuels are typically not properly accounted for in domestic oil demand statistics because of incomplete port reporting and because the fuels are consumed at sea.

At finer geographical and temporal scales, the results indicate an own-price elasticity of −0.14 for the Port of Singapore. This result is consistent with the previous literature (ranging from −0.45 to −0.01) and shows that demand has low sensitivity to price changes, further confirming that marine transport is the most competitive long-distance mode and thus can effectively absorb price fluctuations. However, estimated own-price elasticities were not significant for Panama or the Port of Seattle–Tacoma.

2.2 HTL OF BIOMASS

HTL is a process of depolymerizing biomass (i.e., biocrude) into a liquid biocrude oil under higher pressures and moderate temperatures. A key feature of HTL is the use of water (and catalysts) to promote the depolymerization reactions. Thus, HTL is uniquely suited for the wet waste feedstocks. The resulting oils (i.e., biocrudes) from this process are characterized by high MWs, low acidity, and high viscosity. To become miscible with distillates and meet ISO 8217 marine fuel specifications, the raw biocrudes must be hydrotreated to remove moisture, inorganics and oxygenates.

The HTL biocrudes evaluated in this study were produced at PNNL, which conducted preliminary analysis on three feedstock HTL conversions with the following hydrotreating strategies (more detailed information is below and Figure 5):

- No hydrotreating (raw biocrude)
- Mild hydrotreating in guard bed (one step)
- Full hydrotreating in a train of guard and main bed (two steps)

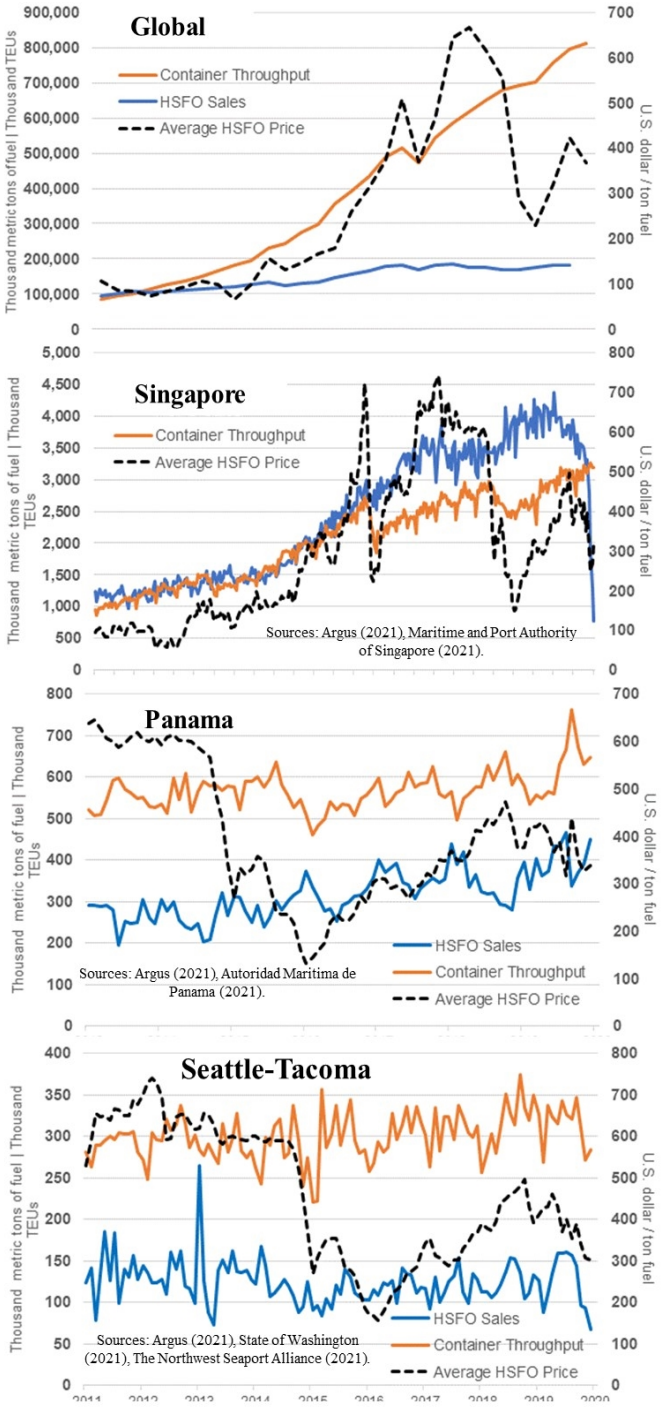

Figure 4. Bunker fuel sales, average marine fuel prices and container throughput globally, and for the Ports of Singapore, Panama, and Seattle–Tacoma.

Feedstocks included the following:

- Sewage sludge (sludge HTL)
- Sludge combined with food waste (FW) and fats/oils/grease (FOG) (50%sludge/ 40%FW/10%FOG HTL)

- Sludge combined with FOG (80% sludge/20% FOG)

Appendix B provides a more detailed assessment of the pathways, variables, and processes used.

The modeling approaches considered HTL runs of wet waste, such as sludge, FW, and FOG waste, to identify the potential opportunities of converting wet waste feedstocks to viable marine fuel. Specifically, the analysis included the following feedstocks and pathways:

- Sewage HTL from the Detroit wastewater treatment plant
- A blend of waste sludge, food, and FOG
- A blend of waste sludge and FOG

These feedstocks correspond to the HTL oils produced at PNNL for physical and chemical analyses.

Figure 5 shows the process configuration used for a HTL pathway, as well as the potential minimum processing requirements for marine fuel blendstocks. Here, the waste HTL processing plant is sited at the wastewater treatment plant. Biocrude upgrading is also co-located with the HTL plant in this scenario (i.e., no transportation cost for biocrude). The key process technical assumptions associated with HTL of different feedstocks are summarized in Table A.1.

Plant scale is a key economic driver for making these pathways feasible because production costs almost always decrease with increasing scale. A preliminary wet waste resource analysis shows that 82% of the total wet waste resources in the United States could be collected at sites over a 1,000 dry ton/day scale at a transportation cost of $50/MT (based on 2014 transportation costs) (Mulchandani 2016). To take advantage of economies of scale, a large HTL plant at a scale of 1,000 dmtu/day was modeled and evaluated. Another strategy to reduce cost is to reduce the number of processing steps by removing hydrocracker unit and simplifying hydrotreating steps since the raw or mildly hydrotreated biocrude could be blended with existing maritime fuels. This hydrotreating equipment includes a guard bed for metals and mild heteroatom removal and a main hydrotreating reactor for removing most of the bound oxygen, nitrogen, and sulfur. Different hydrotreating steps would likely be required for different wet wastes because of the variability of feedstock compositions.

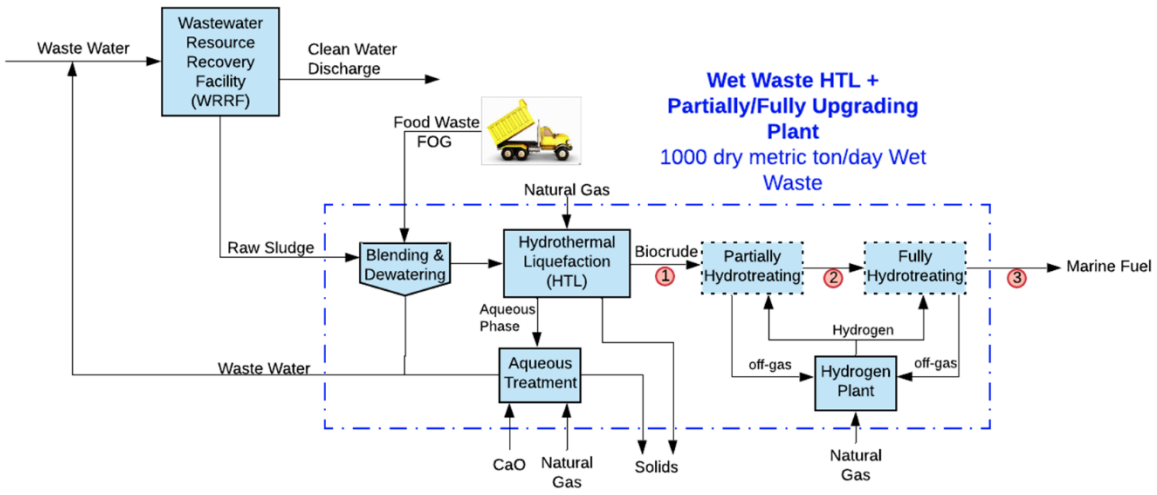

Figure 5. The potential sampling locations for the biocrude/bio-oil for marine fuel analysis.

The minimum fuel selling price (MFSP) was determined using a discounted cash flow analysis, which is a valuation method used to estimate the value of an investment based on its projected future cash flows. In this study, all costs are in 2016 US dollars.

Table 1 lists the modeled biocrude MFSP from sludge HTL, sludge/food/FOG HTL and sludge/FOG HTL. Biocrudes derived from sludge/food/FOG and sludge/FOG have a similar MFSP of approximately $1.30/GGE, whereas biocrude from sludge HTL has a relatively higher MFSP of $1.51/GGE. All the modeled biocrude MFSPs are lower than the reported VLSFO price ($1.78/GGE). These results show that feedstock type has enormous influence on the processing costs. This effect is attributed to variation in feedstock composition (e.g., lipid, protein, and carbohydrate) and HTL operating conditions such as feed solid content. Biocrude yield is a significant economic driver since high lipid content will increase the biocrude yield, and high levels of solid matter in the feedstock will reduce capital costs of the HTL reactor.

Table 1. Economic summary of HTL biocrude of three feedstocks

Parameter	Sludge HTL	50% sludge/40% food/10% FOG HTL	80% sludge/20% FOG HTL
Avoided disposal credits ($/dmtu)	200	107	50
Transportation cost ($/dmtu)	50	50	50
Biocrude MFSP without potential credits ($/GGE)	1.51	1.27	1.30
Biocrude MFSP with potential credits ($/GGE)	0.18	0.78	1.30
Biocrude MFSP contribution ($/GGE)			
Feedstock potential credits	1.33	0.49	0.00
Operating cost	0.71	0.57	0.56
Capital cost and taxes	0.80	0.70	0.74
Feed solids (wt %)			
Ash included	20	25	17
Ash-free	15	21	17
Biocrude yield: dry, ash-free (wt %)	44	46	50
Biocrude production (mmGGE/year)	31.2	33.8	35.8
Total installed equipment cost ($MM)	105	96	108
Total capital investment ($MM)	210	192	215

dmtu: dry metric ton; GGE: gasoline gallon equivalent

This analysis does not consider the potential avoided disposal costs for the wet waste. For example, the sludge management and disposal costs account for about 40%–65% of the total wastewater treatment plant's operating expenses. The common routes of sludge management include land application, landfill-based disposal, and incineration. The solids reduction resulting from the HTL process would conceivably result in significant savings in avoided disposal costs to the plant. In fact, the numerous sources indicate a wide range of the sludge disposal credits ($200–$800/dry ton) depending on the management practice, location and policy, and so on (Seiple et al. 2020; Mulchandani et al. 2016).

A recent national analysis shows that national sludge weighted price is around $200/dmtu and FOG price is around $551/dmtu (Badgett et al. 2019). For a conservative analysis, $200/dmtu sludge can be used as an avoided disposal cost. Similarly, food waste is typically discharged to anaerobic digestion plants for producing methane and the average tipping fee is $157/dmtu based on a recent EPA report (EPA 2021).

With reductions in wet waste price and potential transportation cost, the MFSPs for the three feedstock scenarios could be lower as shown in Table 1. The properties of these biocrudes are listed in Table B.2.

2.2.1 Economic Impact of Upgrading/Hydrotreating HTL Oils

Table 2 lists the modeled MFSP of partially and fully hydrotreated fuel from three feedstocks and their cost allocations. Fully hydrotreated fuel has lower sulfur (10-50 ppm) and oxygen content (<1.0%) than that in the partially hydrotreated fuel (S < 0.5%, O < 5.0%), and the oxygen and sulfur content in the finished oil can be controlled by adjusting the operating condition such as space velocity, temperature, and pressure. As expected, MFSPs for the fully upgraded fuel are higher than the partially upgraded fuel MFSPs because of the addition of natural gas, and because the additional energy/material requirements add hydrogen and remove oxygen. As shown in Table 2, producing fully upgrading fuel increases the modeled MFSP by $0.19/GGE on average for the three feedstocks. Additionally, feedstock cost is the largest contributor to the MFSP of partially and fully upgraded fuel.

Table 2. Economic summary of partially and fully hydrotreated fuel from three feedstocks

Parameter	Sludge HTL		Sludge/food/FOG HTL		Sludge/FOG HTL	
	Partially	Fully	Partially	Fully	Partially	Fully
MFSP ($/GGE)	2.09	2.25	1.81	2.01	1.83	2.04
MFSP contribution ($/GGE)						
Feedstock cost	1.61	1.63	1.34	1.37	1.37	1.40
Operating cost	0.24	0.29	0.24	0.30	0.23	0.30
Capital cost and taxes	0.24	0.33	0.23	0.34	0.23	0.34
Total installed equipment cost ($MM)	35	49	35	50	37	53
Total capital investment ($MM)	70	97	70	100	74	106

2.3 OILS DERIVED FROM FAST PYROLYSIS OF BIOMASS

Bio-oils are derived via fast pyrolysis of biomass, which can range from forest products to corn stover. During pyrolysis, the feedstock is rapidly heated to approximately 500°C for 1 to 2 s, and the gases are then cooled to form a liquid fuel (i.e., bio-oil) with high water and acid contents. To achieve suitable yields and quality, the feedstocks must be dried to moisture contents below 5%. This process adds to the overall cost. The aqueous phase of the condensed pyrolysis product is removed, and the remaining product is an oily, water-insoluble, highly polar and acidic fraction that requires further upgrading/hydrotreating to remove water and oxygenates, thereby improving combustion quality and enabling blending with distillates. This process is energy-intensive and expensive, and therefore, upgraded bio-oil is not an economically feasible option for distillate fuels. However, because large two-stroke crosshead marine engines can operate on poorer combustion quality fuels than conventional diesel engines, bio-oils may have utility as a marine fuel. Key concerns include whether raw bio-oil can be used in marine applications, economic and environmental benefits, blend stability with HFOs, compatibility with fuel handing infrastructure, and suitable combustion quality.

2.3.1 Approach

In this study, two promising production pathways (developed by researchers at NREL) were evaluated French et al. 2021, Iisa et al. 2017). These pathways are listed as follows and differ primarily in the catalyst chemistries used in upgrading. Further details are included in Appendix C

- Pathway 1: An ex situ catalytic fast pyrolysis (CFP) approach with vapor phase upgrading over a Pt/TiO_2 catalyst and with whole bio-oil and lighter cuts removed. This pathway also includes a 2030 projection on increased yield of the bio-oil product.

- Pathway 2: An ex situ CFP with vapor phase upgrading over a ZSM-5 catalyst and with whole bio-oil and lighter cuts removed.

A simplified process flow diagram for these two pathways is shown in Figure 6.

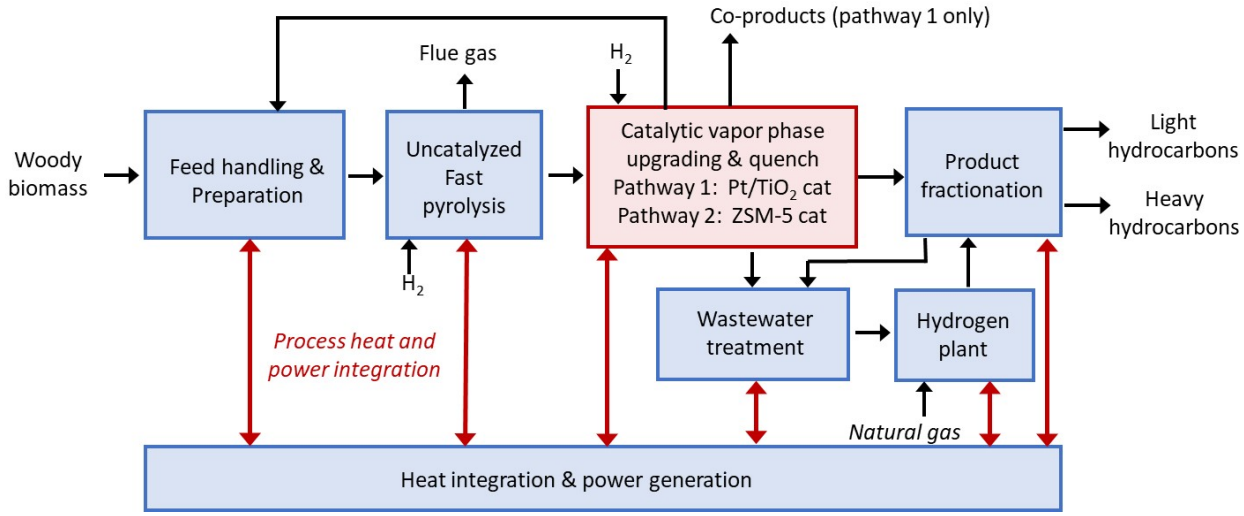

Figure 6. Main process steps for Pathways 1 and 2. Note that the key difference is that Pathway 2 does not produce any saleable coproducts.

Pathway 1

The ex situ CFP vapor phase upgrading over a Pt/TiO_2 catalyst pathway was developed based on a recent study (Griffin et al. 2018) that did not include the downstream hydrotreating steps and included whole bio-oil and lighter cuts as the hydrocarbon blendstocks for marine propulsion. This pathway also includes a high bio-oil (>60%) yield scenario (i.e., 2030 projection). The feedstock for the pathway is a 50/50 blend of forest residues and clean pine. All plants are based on a 2,000 MT/day feedstock rate. The process model for uncatalyzed fast pyrolysis uses a circulating fluidized bed design. The dual-bed reactor system includes a riser reactor for fast pyrolysis and a char combustor to heat circulating sand to provide the reaction temperatures at 500°C. The solids are removed via cyclones and a hot gas filter. The hot gas filter is required to prevent plugging of the fixed bed ex situ catalytic vapor upgrading reactor with Pt/TiO_2 with 0.5 wt % Pt loading. The ex situ reactor is maintained at 400°C with a biomass-to-catalyst ratio of 12:1. The reactor configurations are shown in Figure 7 (Griffin et al. 2018).

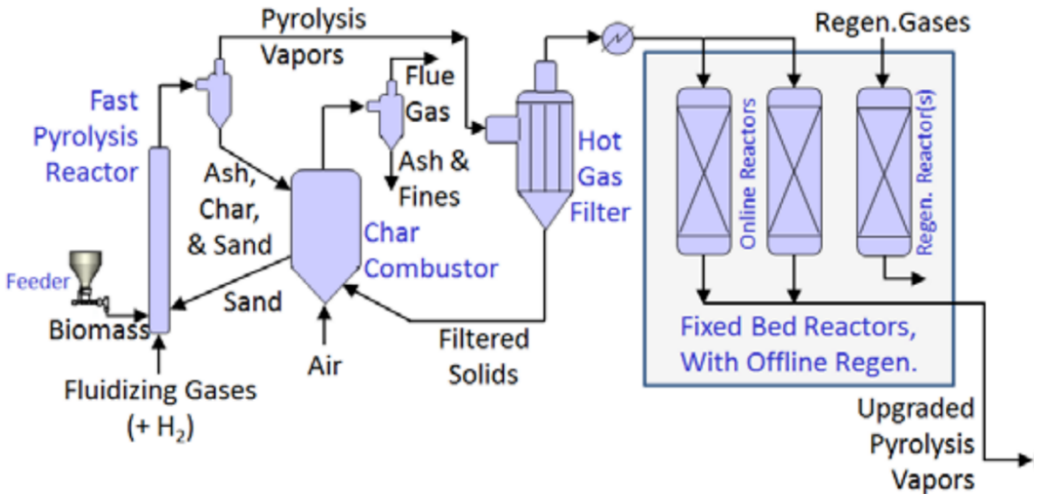

Figure 7. Fast pyrolysis and vapor phase upgrading with Pt/TiO_2.

After vapor phase upgrading via the catalyst reactor, the vapors are cooled via an indirect heat exchanger to the dew point of the vapor stream. The heavy organic bio-oil is condensed in an absorber/condenser with product from a downstream condenser used as the quench liquid. The uncondensed vapors from the first absorber/condenser are sent through another set of heat exchangers before entering a second absorber/condenser column for a final quench. The bottom product from the second condenser is separated into an aqueous stream and sent to the wastewater treatment.

In this exercise, the oil fractions are further evaluated as a whole and two-cut approach. The whole-oil approach considers that all of the bio-oil is treated to make a marine fuel, whereas in the two-cut approach, only the heavier fraction is considered for marine use. The lighter fuel fraction is used in product manufacturing or as a distillate fuel.

For the whole-oil consideration approach, the heavy hydrocarbon stream from the first condenser and the light hydrocarbon stream from the second condenser are combined. For the two-cut approach with the lighter cuts removed, the product streams are kept separate and sold as two distinct products.

For the two-cut approach, the recovery of light oxygenates from the gaseous stream of the second condenser was performed. The oxygenate stream was sent to an adsorption system to remove the light oxygenates, and the stream was sent through a series of distillation columns to recover acetone and 2-butanone (MEK) as saleable products. The overall yield on a mass basis (mass bio-oil/mass biomass feedstock) for the base Pt/TiO_2 case is 23%, with the 2030 projection case being 31%.

Pathway 2

A shown in Figure 6, Pathway 2 is similar to Pathway 1, but whereas Pathway 1 used a fixed-bed reactor, a fluidized-bed reactor is used for Pathway 2. Furthermore, Pathway 2 does not employ hot gas filtration. Instead, the hot pyrolysis vapor stream exiting the uncatalyzed fast pyrolysis reactor is sent directly to the fluidized bed that uses a ZSM-5 catalyst for upgrading.

As with the Pt/TiO_2 case (Pathway 1), the vapors enter the ZSM-5 catalytic upgrading step at 500°C. The upgraded vapors leave the riser reactor, and any solids and spent catalyst material are removed via a cyclone separation process. The spent catalyst is sent to a regeneration reactor that uses air to burn off any coke or char residue from the reactor. The vapors from the catalyst regenerator are sent through a cycle to remove any char or ash. The off-gases from the regenerator are used for hydrogen and steam generation.

All three reaction systems are operated at 500°C. Because of the nature of the products produced from the ZSM-5 catalyst, no coproducts of acetone or MEK are formed. The reactor configurations for this pathway are shown in Figure 8.

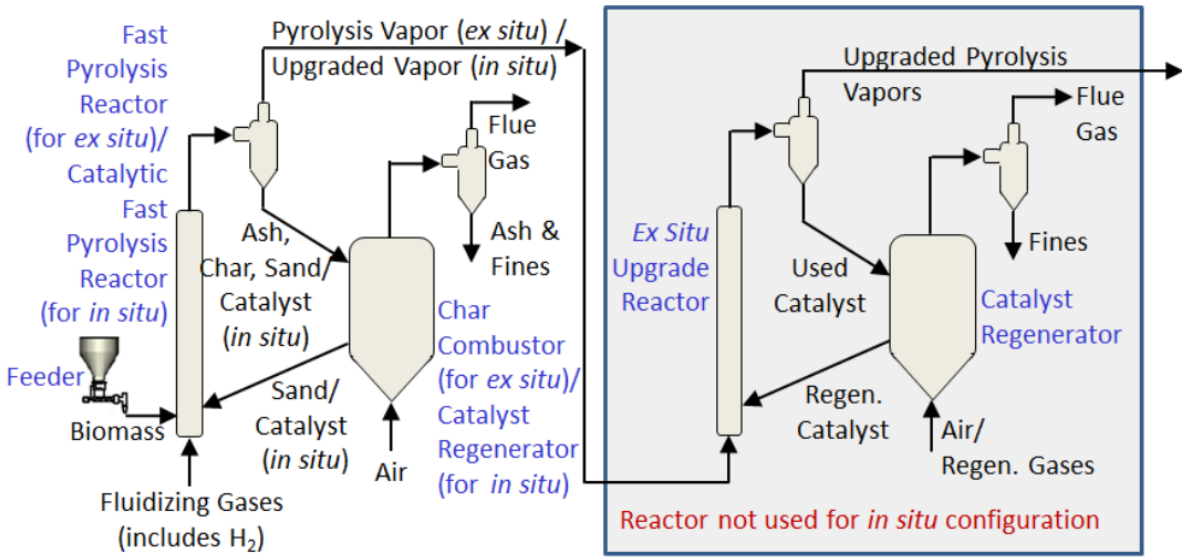

Figure 8. Fast pyrolysis and vapor phase upgrading with ZSM-5.

Again, for the whole-oil production, the light and heavy hydrocarbon streams are combined to maximize the energy content of the bio-oil.

2.4 FT MARINE FUEL DERIVED FROM RENEWABLE LANDFILL GAS

The pathway evaluated for FT production uses landfill gas (LFG) emissions (primarily methane) as a feedstock. These emissions are collected and then processed using steam methane reforming, followed by fuel production via FT synthesis to hydrocarbon blendstocks. A simplified block diagram of this process is shown in Figure 9. Unlike natural gas, LFG contains impurities (such as siloxanes) and approximately 40 vol % CO_2.

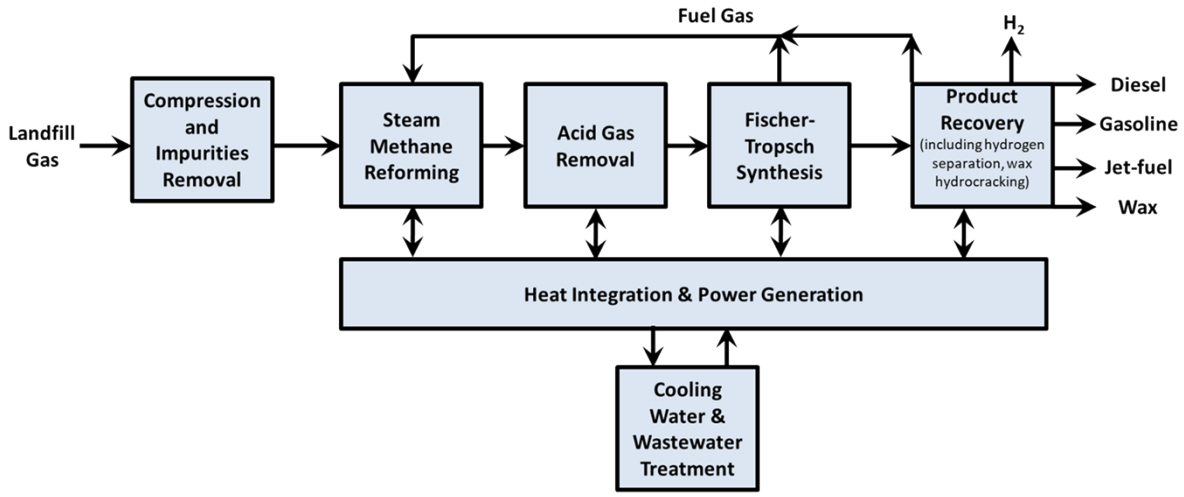

Figure 9. Main process steps for FT production.

FT synthesis is a catalytic conversion process, which converts the synthesis gas to a mixture of reaction products such as diesel, gasoline, jet fuel, and wax products. The overall reaction involved in the FT synthesis is governed by the following general reaction:

$$(2n + 1)H_2 + nCO \rightarrow C_nH_{2n+2} + nH_2O$$

The FT polymerization process offers the ability to produce liquid hydrocarbon fuels with relatively low sulfur and aromatic contents and a more controlled final chemistry than other pathways. Here, the H_2/CO ratio entering the FT reactor was maintained at 1.5:1 by sending a portion of the synthesis gas stream to a pressure swing adsorption system with the off-gas feeding the FT reactor. The effect of the lower H_2/CO ratio results in a less than stoichiometric ratio being fed to the reactor, and thus, only 78% of the CO is consumed in the FT reactor, compared with a typical natural gas feedstock that has an 85% conversion of CO.

The FT products are condensed and separated through a multi-cut distillation column to separate the product streams. The purified H_2 from the pressure swing adsorption system is used for hydrotreating distillation products to yield blendstocks for gasoline, diesel, and jet fuel. Wax produced from the hydrocracker is sold as a coproduct. Any excess H_2 not consumed for hydrotreating, or hydrocracking, is sold as a coproduct. The high CO_2 content in LFG causes a low heating value (relative to natural gas), and therefore, the fuel yields will be lower than natural gas. Further approach details are included in Appendix D.

2.5 LIGNIN ETHANOL OIL BASED ON A LIGNOCELLULOSIC ETHANOL BIOREFINERY AND STAND-ALONE LEO PLANT

NREL researchers developed and evaluated a lignin ethanol oil (LEO) concept that builds on an existing cellulosic ethanol pathway (Humbird et al. 2011) for techno-economic and life cycle analyses. This second-generation ethanol biorefinery produces both ethanol and lignin and allows for the integration of lignin-ethanol solvolysis. Figure 10 depicts the simplified flow diagram of the overall process. The lignin stream, which is a waste stream typically burned for heat and power, undergoes solvolysis to create a reductive environment for depolymerization of the feedstock to biofuels. Supercritical ethanol exists at temperatures exceeding 240°C and pressures exceeding 61 bar. For this pathway, the ethanol loading is set at 9.0 L/kg lignin (or 7.1 kg/kg), and the residence time is 3 h. Ethanol is converted to CO and CO_2, and the unconverted ethanol is recycled, resulting in a net ethanol consumption of approximately 34 g of

ethanol per kilogram of LEO product. The technology does not involve catalysts, and no further hydrotreating is required. Approximately 53% of the dry lignin stream ends up in the LEO product, which is mainly a mixture of monomeric and dimeric lignin species and oligomers, corresponding to a lower heating value of 24.3 MJ/kg, and the residual solids are sent to the boiler. Natural gas is the supplemental fuel required for generating heat and power to meet the biorefinery demand. No excess electricity is produced.

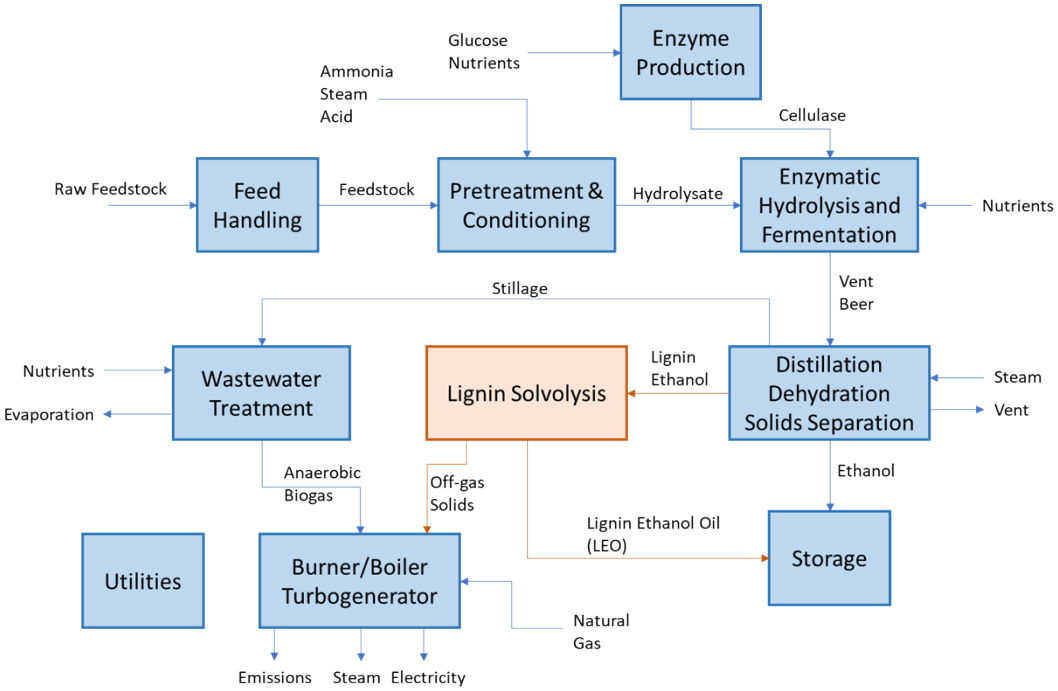

Figure 10. Simplified flow diagram of the integrated ethanol and LEO process.

2.6 SUMMARY OF TEA RESULTS

The economic analyses were conducted by research teams at PNNL and NREL. Specific details concerning the assumptions, variables, and approaches are provided in Appendix B. The PNNL research efforts focused on the HTL production approaches described previously, whereas the NREL researchers studied pyrolysis oils, FT diesel, and LEO. A chart summarizing the TEA results is shown in Figure 11. More detailed descriptions of these analyses are presented in Appendix B, Appendix C, and Appendix D. Figure 11 shows that the MSFP of the HTL oils compare favorably to the two baseline fuels. The modeled CFP bio-oils exhibit higher MSFPs than the baseline fuels, but projected costs for Pathway 1 (CFP Pt/TiO_2) and the FT diesel are encouraging and show that the production costs can approach that of the baseline fuels. LEO produced from an integrated process was shown to be the least economically feasible option, but that LEO becomes more economical if the ethanol component could be added. These cost analyses are highly preliminary and are being refined as more information is provided concerning biofuel efficacy and production needs.

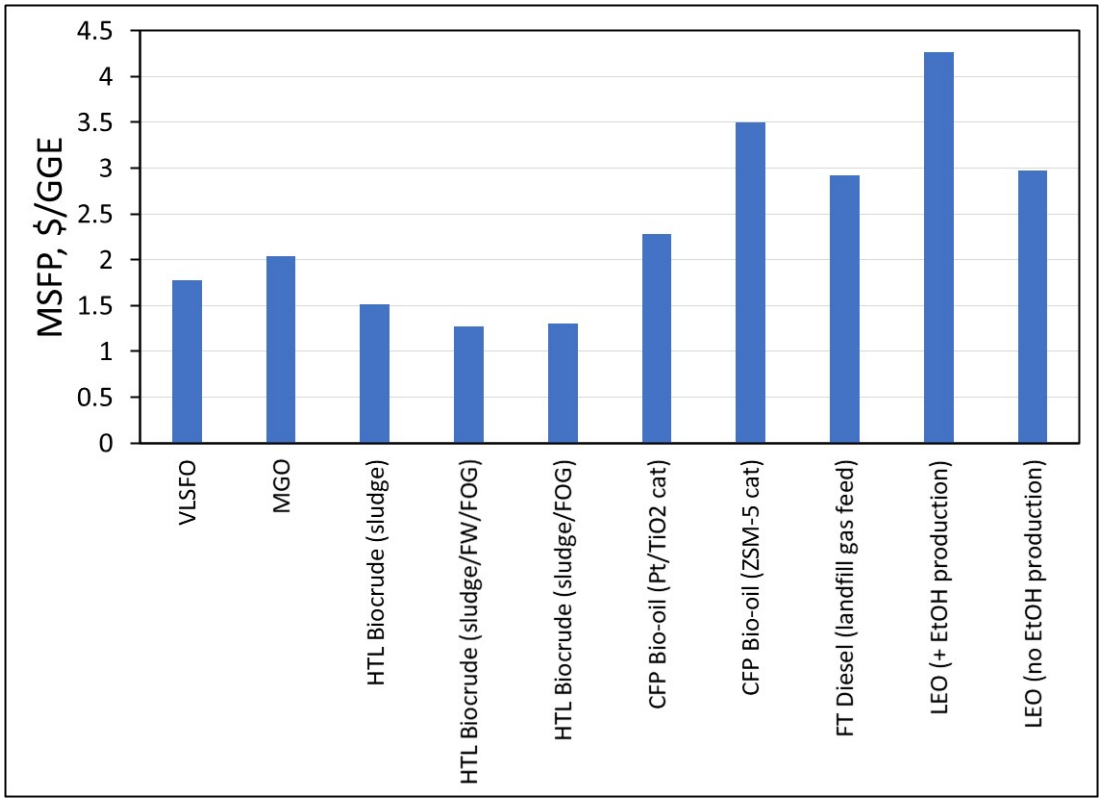

Figure 11. TEA summary ($/GGE). For each ex situ CFP pathway, the corresponding MFSP for both whole oil and lighter cuts are identical as MFSPs were determined based on the total fuel energy produced.

2.7 CFP BIO-OIL SAMPLE PRODUCTION

The economic

3. SUSTAINABILITY ANALYSIS

3.2 UPDATES TO THE MARINE MODULE IN ARGONNE'S GREET MODEL

Several enhancements and developments have been made to Argonne's GREET Marine module. These include the development of marine ammonia, e-methanol, e-FT fuel, and HFO with sulfur scrubber pathways. These pathways link upstream life cycle inventory for feedstock and fuel production with downstream use in marine engines and vessels. An overview of GREET's marine fuel pathways is provided in Appendix E.

3.3 ENVIRONMENTAL ANALYSIS

The International Maritime Organization (IMO), the governing body of international shipping, have set aggressive targets aimed at reducing the carbon intensity of maritime vessels, with an overall goal of a 50% reduction in greenhouse gas emissions from international shipping by 2050, relative to 2008 levels, and pursing efforts to phase out GHG emissions from marine shipping by the end of this century[3]. These regulations are driving shipowners and operators to diversify their fuel portfolio to consider low-carbon alternatives, and thus provides a unique opportunity for the expanded use of biofuels in the maritime sector.

In this work, LCA was conducted using Argonne's GREET model, utilizing process model simulation output provided by NREL and PNNL. This approach translates process material, energy consumption, utility requirements and emissions reported in process simulation models into broad-based impacts on the environment, and thus provides a scientifically rigorous basis for estimating and ranking the environmental sustainability of emerging marine fuel pathways. Consequential LCA was performed for HTL and waste-to-energy pathways (listed in Table E.2). This consequential perspective considers the counterfactual scenario for waste-to-energy systems, representing the fate of the waste stream under current waste management practices. For example, in LFG-to-fuel systems, if LFG is diverted from flaring and is instead used to produce marine fuels, the waste-to-energy system would be accredited with the avoided emissions that would have otherwise occurred due to biogas flaring. Thus, consequential LCA can pride a novel and complementary perspective on the environmental performance of marine waste-to-energy systems, and in select cases, these consequential results can identify opportunities leading to net negative emissions relative to standard waste management practices.

Figure 12 plots the life cycle GHG emissions for the selected marine biofuel pathways. Fuel pathways are sorted from highest to lowest GHG emissions, and the stacked bars denote the contribution of feedstocks, material, and energy use to the overall life cycle GHG emissions. Positive values indicate GHG emissions that occur throughout the supply chain, and negative values indicate displacement credits, counterfactual credits, or carbon sequestration that occurs in the supply chain. The black circles represent the well-to-hull GHG emissions, the dashed black line represents a 50% GHG reduction relative to HFO (in line with the IMO's GHG targets), and the dashed red line represents a 70% reduction (representative of recent emissions targets set by DOE's Bioenergy Technologies Office [BETO]). These results are compelling, with GHG emissions ranging from 33 to -44 gCO_2e/MJ over the host of pathways considered. For CFP pathways, analysis reveals that the impacts for procuring woody biomass and the use of process natural gas are the largest contributors to overall GHG emissions. CFP pathways also receive a large coproduct credit for the produced acetone, MEK, and electricity. In waste-to-energy systems, electricity, chemicals (quicklime), and natural gas use are the primary contributors to overall life cycle GHG emissions. Waste-to-energy pathways demonstrate low carbon intensities and in select cases are carbon negative, but they are sensitive to the choice of counterfactual waste management scenario. For example, FW pathways demonstrate a negative carbon intensity, primarily because of the large negative counterfactual credit. This credit is a result of the higher rate of methane formation from landfilling of FW, which results in comparatively higher fugitive emissions of biogenic methane per unit waste relative to the other waste-streams. Therefore, avoiding fugitive biogenic methane emissions from FW results in a large counterfactual emission credit. In other instances, such as wet waste sludge, which is traditionally managed using anaerobic digestion, the business-as-usual waste management system produces electricity and other value-added coproducts. Therefore, avoiding the generation of these value-added coproducts results in a positive emissions burden for the HTL system.

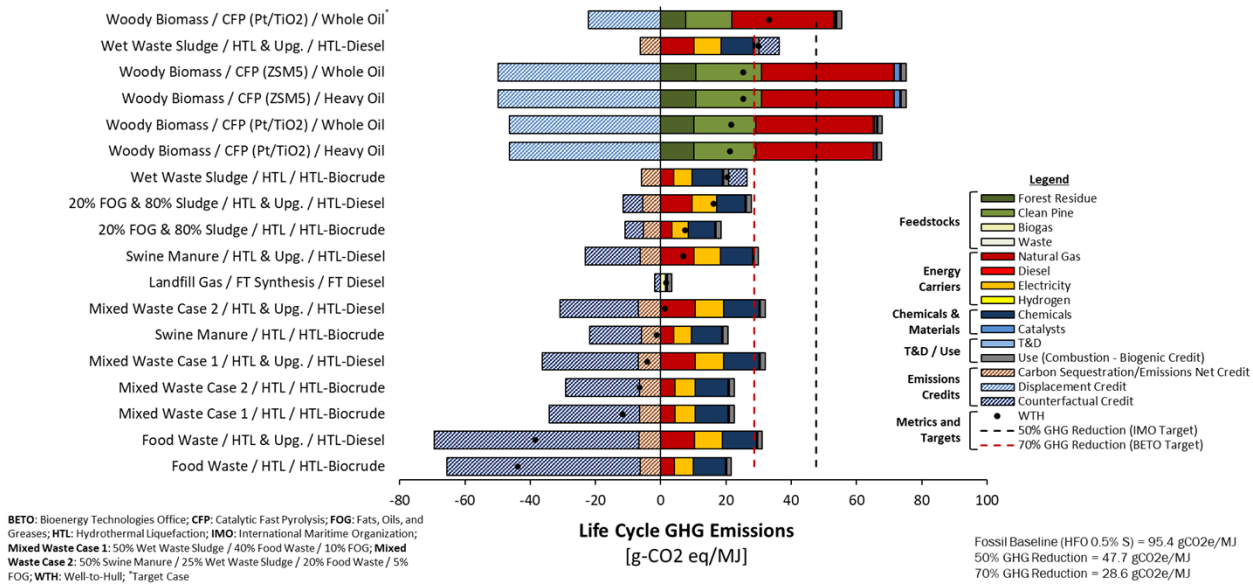

Figure 12. Life cycle GHG contribution analysis for 18 marine fuel production pathways.

Figure 13 shows an environmental "heat map," highlighting the percentage change in life cycle environmental impact categories relative to HFO (0.5% sulfur). For example, HTL-biocrude from FW yields a 146% reduction in life cycle GHG emissions relative to HFO. Results are shown for select marine biofuels as well as fossil fuels. Values in green denote a reduction in emissions relative to HFO, values in yellow indicate similar performance (or marginal change) relative to HFO, and values in red indicate higher emissions or impacts relative to HFO. Results indicate that marine biofuel pathways demonstrate greater than 50% reduction in life cycle GHG emissions relative to HFO, and thus are commensurate with the IMO's long-term GHG emissions targets. In addition, biofuels generally exhibit low GHG, SO_X, and particular matter emissions, but in select cases, they may demonstrate higher water use relative to HFO (0.5% sulfur).

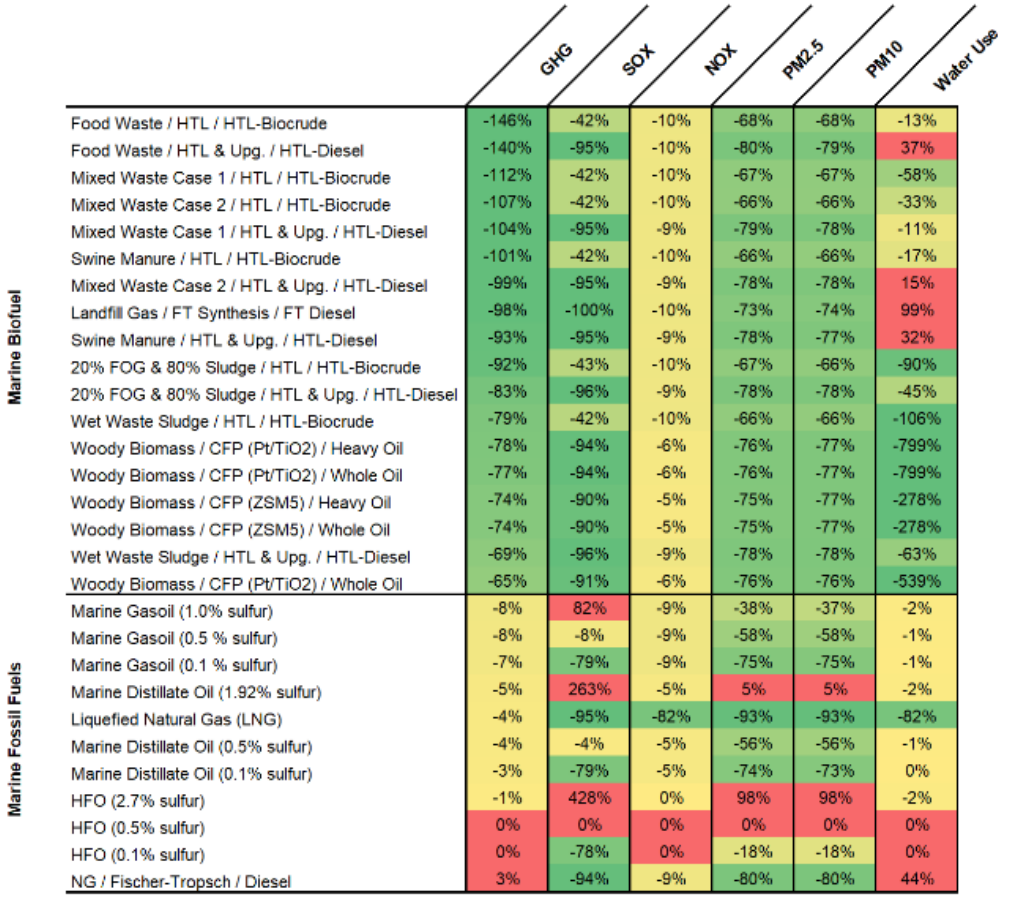

Figure 13. Environmental heat map. PM: particulate matter.

Future work will explore several sensitivity cases and the effects of the coproduct handling method (e.g., allocation scheme, displacement) on overall LCA results.

4. FUEL SAMPLE PRODUCTION

Fuel samples of HTL biocrudes and bio-oils were produced for experimentation and provided to ORNL. The HTL biocrudes were provided by PNNL and were derived from algal and waste sludge feedstocks. They include the following:

- Biocrude (algal feedstock)
- Biocrude bottom (heavy MW cut) (algal feedstock)
- Biocrude upgrade or distillate cut (algal feedstock)
- Biocrude (sewage feedstock)
- Biocrude (wood waste composite feedstock)
- Biocrude (wood bulk, sulfided feedstock)

4.1 CFP BIO-OIL SAMPLE PRODUCTION, ANALYSIS, AND TESTING

The bio-oils samples were provided by NREL and include the following:

- 7195-077 B:C 6 CFP oil: a CFP oil prepared over a Pt/TiO_2 catalyst
- 7070-34-5 FP first condenser oil: a heavy fraction of non-CFP oil (separated by fractional condensation during pyrolysis)
- 7070-34-10 CFP first condenser oil: a heavy fraction of CFP oil prepared over a Pt/TiO_2 catalyst (separated by fractional condensation during catalytic pyrolysis)
- A non-CFP oil
- A CFP oil prepared over a ZSM-5 catalyst

With the exception of the CFP-ZSM-5 oil, the oils were produced in NREL's bench-scale 2-inch fluidized bed reactor system using a mixture of 50% clean pine and 50% forest residues as feed. The high-boiling fractions of the FP and CFP-Pt/TiO_2 oils were produced by fractional condensation with the heaviest (highest boiling fraction) selected for marine fuel evaluation; the aim is to use the lower-boiling fractions for other fuels, e.g., sustainable aviation fuels, or co-products generation. The CFP-ZSM-5 oil was produced in in NREL's pilot plant using 100% clean pine. More details on the oil production methods can be found in the literature (Griffin et al. 2018, Iisa et al. 2017, French et al. 2021, Smith and Gaston, 2019) [ref].

The pyrolysis oils were analyzed for carbon and hydrogen by a LECO combustion analyzer, for water by Karl Fischer titration, for sulfur and metals by Inductively coupled plasma analysis (ICP), for ash and volatility by simulated distillation- thermogravimetric analysis, and chemical composition by gas chromatography mass spectrometry coupled with a Polyarc converter and a flame ionization detector (GC-MS-FID Polyarc)[3]; see Figure 14 and Table 3 for summaries of the results. All oils had low sulfur contents (15-77 ppm or 0.0015-0.0077 wt%), vastly below the IMO 2020 low-sulfur requirement. However, the water and acid numbers were high and do not meet ISO 8217 specifications. The water contents varied from 3.5 to 16 wt% while the specifications establish upper limits of 0.5 vol%. The carboxylic acid numbers (acid number, which accounts only for carboxylic acids, not for phenolics) were >50 for the fast pyrolysis oils and 24-29 for the CFP oils vs. 0.5 limit for distillate marine fuels and 2.5 for residue marine fuels). In order to be able to blend the pyrolysis oils with fossil marine fuels at meaningful fractions further upgrading of the oils will be needed. These could include a different fractional condensation system, extraction to remove water and acids, or mild hydrogenation, which are all proposed to be studied in future projects.

Table 3. Summary of pyrolysis oil analytical results.

FP oil	FP oil heavies	CFP (ZSM-5)	CFP (Pt/TiO_2)	CFP (Pt/TiO_2) heavies

C, wt%	48	49	66	75	73
H, wt%	7.5	6.9	7.3	7.9	8.3
O, wt%	45	44	27	17	18
H_2O, wt%	16	12	11	3	7
Ash, wt%	<0.5	<0.5	1	<0.5	<0.5
S, ppm	15	29	77	19	19
CAN*, mg KOH/g	58	70	26	29	24
wt% residue >550°C	18	21	26	11	8
wt% boiling <350°C	65	65	49	69	76

* Carboxylic acid number

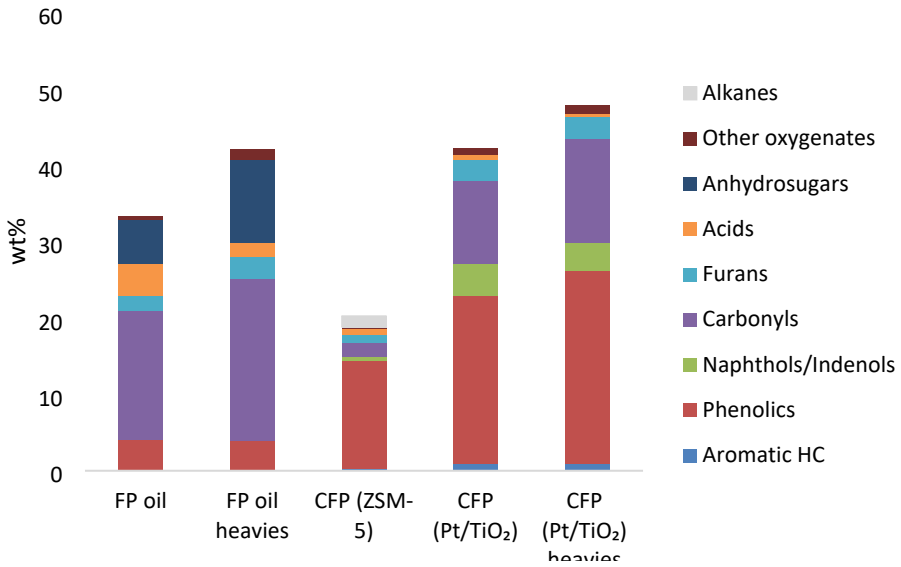

Figure 14. Summary of GC-MS-FID Polyarc analysis of pyrolysis oils.

5. STABILITY, RHEOLOGY, AND COMBUSTION STUDIES ON BLENDS WITH VLSFO

The ASTM D4740 test was conducted on the biocrudes, and asphaltenes precipitated in VLSFO at concentrations of >10 wt %. The biocrude upgrade and biocrude algal were further evaluated for viscosity and combustion properties. Prior analysis of biocrude showed that it predominantly comprised of high-MW components; therefore, it likely has relatively low polarity. The addition of fuel chemistries with low polarity to a residual fuel oil is known to promote asphaltene precipitation.

The algal biocrude and the biocrude upgrade samples were evaluated for viscosity behavior as blends with VLSFO. In each case, the blend level of the biocrude was 5 wt %. The viscosity curves for these blends were measured at 25°C, 50°C, and 90°C and are shown in Figure 15 alongside the neat VLSFO. As shown in the figure, the addition of 5% biocrude significantly affected the viscosity of VLSFO. The viscosity of neat VLSFO decreased with increasing shear rate, whereas the viscosity of the blends containing algal biocrude or the biocrude upgrade were relatively constant over the range of shear rates.

For each temperature, the viscosity of the samples containing the biocrude upgrade were lower than for the raw biocrude. At low shear rates, the samples with the addition of 5% algal biocrude (or biocrude upgrade) has much lower viscosities than for the neat VLSFO. At 25°C, the samples containing the biocrudes had higher viscosities when the shear rate exceeded 10/s. At all test temperatures, the viscosities of the blends containing algal biocrude or the biocrude upgrade were lower than VLSFO for the range of shear rates tested. As shown in Table 4, the raw biocrude had a lower energy density than VLSFO, which was expected given the oxygen atoms in the raw biocrude. The upgraded distillate and bottom cuts had higher energy content that VLSFO, but the oxygen was removed, which improves the energy density of the fuel cuts.

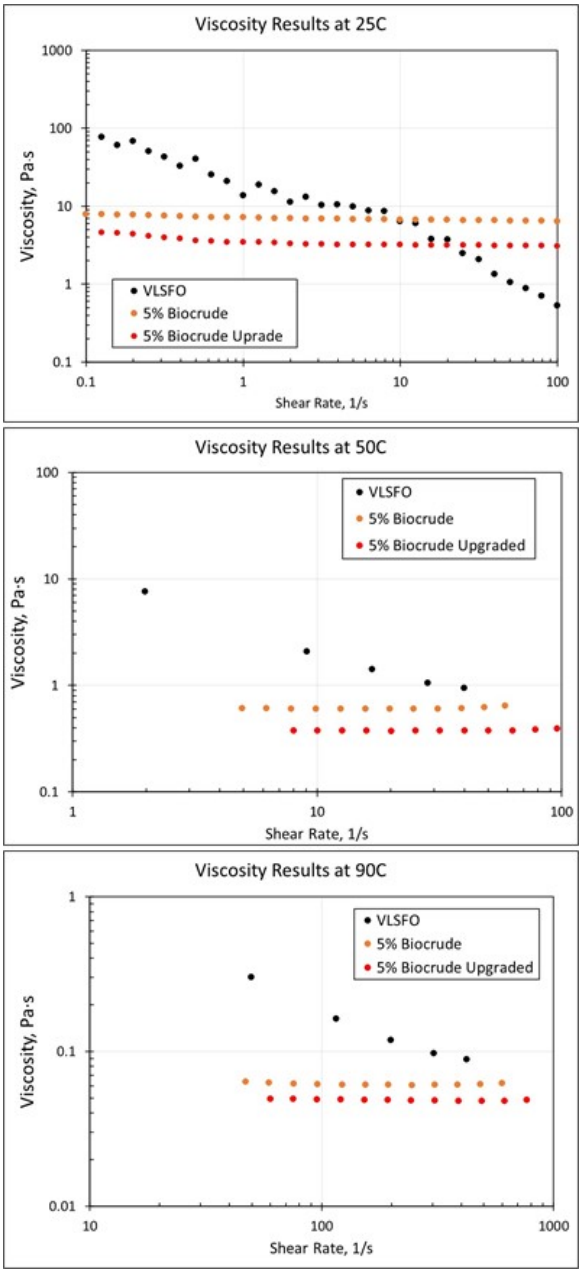

Figure 15. Viscosity results of biocrude blends with VLSFO as a function of temperature and shear rate.

Table 4. Heat of combustion results for tested biocrudes (ASTM D240N)

Fuel sample	Heat of combustion	
	Gross (MJ/kg)	Net (MJ/kg)
VLSFO	42.79	40.61
Algal biocrude	33.53	31.39
Algal biocrude upgrade (bottom)	44.73	42.11
Algal biocrude upgrade (distillate)	45.72	42.82

The ignition quality of the test fuels was determined using the standard test method, IP 541/06: Determination of ignition and combustion characteristics of residual fuels – constant volume chamber method. These results are shown in Figure 16, while the ASTM D240N heat of combustion results are shown in Table 5. As shown in the figure, the rate of heat release (ROHR) profiles show that the biocrude additions did not significantly affect the combustion profiles of VLSFO. The test results included written designations that the biocrude additions would be suitable for use in marine engines. Although the influence of biocrude on the combustion performance was minor, some notable and important observations are shown in Table 5. For instance, the blend containing 5% raw biocrude produced a small dip in the estimated cetane number compared with neat VLSFO. This result is attributed to the presence of oxygenates in the biocrude, which reduce the energy density; also, the biocrude contains a heavier MW fraction that is not as readily combustible as small MW hydrocarbons that exist in VLSFO. This effect is also responsible for the slight delay in ignition and combustion, and increase in combustion period, which are also shown in the table.

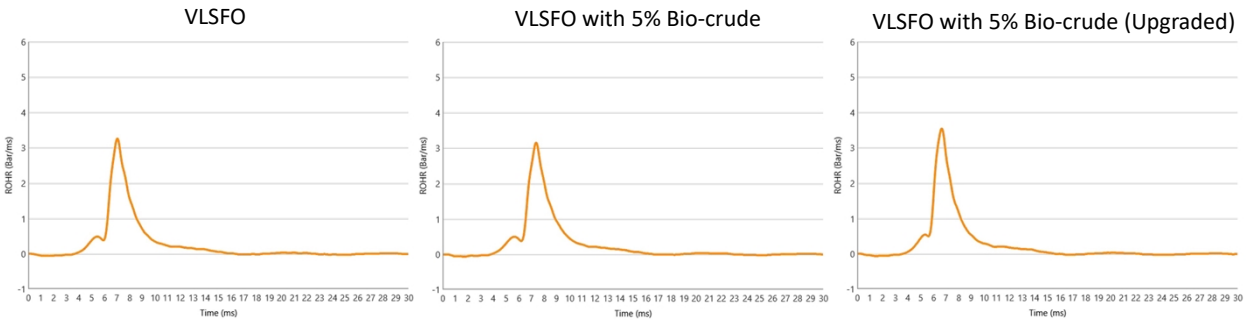

Figure 16. ROHR profiles of VLSFO and its blends with biocrude.

Table 5. Key combustion parameters for VLSFO and its blends with raw biocrude and the biocrude upgrade

Parameter	VLSFO	VLSFO containing 5 wt % raw biocrude	VLSFO containing 5 wt % biocrude upgraded to remove oxygenates (low MW fraction)
Estimated cetane number	24.4	22.9	27.1
Ignition delay (ms)	5.17	5.32	4.71
Main combustion delay (ms)	6.42	6.64	6.05
End of main combustion (ms)	10.73	11.15	10.14
Pre-combustion period (ms)	1.25	1.33	1.34
Main combustion period (ms)	4.32	4.50	4.09
After burning period (ms)	4.49	5.40	4.06
Maximum ROHR level (bar/ms)	3.27	3.16	3.55
Position of max ROHR (ms)	7.12	7.42	6.70

Accumulated ROHR (bar)	7.17	7.28	7.33
Maximum pressure (bar)	7.31	7.42	7.48

During the upgrading process, the composition of the biocrude was separated into the heavier MW fraction and lighter MW fraction. The lighter MW fraction (i.e., the biocrude upgrade) has distillate-like physical properties and was evaluated as a blend with VLSFO. The lighter MW composition (and distillate-like behavior) of the biocrude upgrade is responsible for the reduction in ignition delay, onset of combustion, and reduced combustion period shown in Table 5.

This section summarizes the work conducted on the analysis of biocrude fuel properties toward the suitability as a blend with HFO. HTL biocrude derived from various low-cost wet waste feedstocks (e.g., sludge, FW, FOG) and biocrude sampled at different locations of the processing train (e.g., after HTL, after guard bed, after hydrotreating) were provided to ORNL for the initial screening analysis. The initial results show that biocrude effectively lowers the viscosity of HFO (even at low concentrations) and has good compatibility with fuel system metals. The initial spot test analysis (ASTM 4740) on the biocrude blend stability with HFO shows the formation of precipitates with blend levels as low as 5% biocrude. The particular composition of the biocrude with the asphaltene fraction in the HFO causes the formation of precipitates, which can cause plugging of fuel filters. A study was conducted to evaluate the influence of additives to mitigate asphaltene precipitation. These results are shown in Table 6.

Table 6. Additive impacts on HFO blending spot test analysis on wet waste–derived biocrude

Additive	Biocrude		Hydrotreated biocrude	
	Percentage of blend in HFO (%)	Spot test (pass/fail)	Percentage of blend in HFO (%)	Spot test (pass/fail)
No additive	5	Pass	5	Pass
	10	Fail	10	Pass
	20	Fail	20	Fail
Additive 1	10	Pass	10	Pass
	20	Fail	20	Pass
Additive 2	10	Fail	10	Pass
	20	Fail	20	Fail
Additive 3	10	Fail	10	Pass
	20	Fail	20	Fail
Additive 4	10	Pass	10	Pass
	20	Pass	20	Fail
Additive 5	10	Fail	10	Pass
	20	Fail	20	Fail

As a path to improve the biocrude blend level with HFO, an initial screening analysis was conducted with various fuel additives that are commercially available.

The spot test was conducted based on ASTM D4740, and 0.5% additive was added to the fuel blend at varying compositions. Preliminary results show that the addition of additives can improve the blending limit beyond the 20% level.

6. LOGISTICS

In 2018 global marine fuel use was ~4.3 million barrels per day mostly supplied by HFO and marine gasoil (ABS 2019). U.S. bunker fuel use in 2018 was 150 million barrels which represents 3% of transportation energy use and 1% of U.S. petroleum use (EIA 2019). Very little biofuels are currently used in shipping accounting for 0.1% of fuel use in 2019 (Tattini 2020). The International Energy Agency (IEA) projects low and zero-carbon fuels to account for 3% of international energy consumption in 2030 and about 33% in 2050 based on current policies (Tattini 2020). Between 2020 and 2021, numerous large shipping companies have conducted biofuels trials and no performance issues have been reported.

Large ships have extensive fuel storage systems with capacities capable of propelling the ship for up to 70 days. A ship's refueling system consists of multiple tanks which only store fuel from one source at a time-meaning that if fuel is purchased from two different sources-it will be stored in separate tanks and one fuel is run through the engines at a time. Ships order fuel from marine fuel suppliers and it is delivered by a bunker barge which pulls up alongside the ship in a harbor or offshore. This process can take many hours depending on quantity of fuel delivered. Staff from both a ship and barge oversee the refueling process.

Bunker barges systems for fueling include flexible pipes for receiving fuel from a marine terminal as well as separate pipes for delivering fuel to a vessel, valves, manifolds, pumps, leak detection and containment equipment. Bunker barges have multiple tank and fuel systems to enable them to deliver multiple marine fuel types.

Assuming the biofuel is a biooil similar to the marine fuels used today, there are no anticipated negative impacts for using biofuels in existing ships and fuel bunker barges. Delivery of biofuels is not anticipated to be an issue with existing bunker barges. Cleaning of the ships fueling systems would be necessary as they do with any fuel switching with costs ranging from $250,000 to $500,000 for a bunker barge with capacity of 20,000 to 50,000 barrels. Also, heavy fuel oils use non-mechanical seals which are not used with lighter fuels. Bunker barges would likely need to update sealing equipment to accommodate biofuels.

Industry concerns with a new fuel would be pour point, precipitation, waxing, oxidation of fuel, shelf life as ships store fuel longer than other forms of transportation. If the pour point of a new fuel is higher, fuels must be heated to avoid wax formation and it may be necessary to adjust the temperature settings of the heater. Also, if the new fuel has a lower energy density, centrifuges will need to be recalibrated. If it is determined that a new fuel needs to be purified, the onboard purification system will need to have parameters set for the viscosity of the new fuel. Another related consideration is updating fuel transition clause in charter parties for insurance purposes.

7. REFERENCES

Acosta, M., Coronado, D., & Cerban, M. del M. (2011). Bunkering competition and competitiveness at the ports of the Gibraltar Strait. *Journal of Transport Geography*, *19*(4), 911–916. https://doi.org/10.1016/j.jtrangeo.2010.11.008

Ajanovic, A., Dahl, C., & Schipper, L. (2012). Modelling transport (energy) demand and policies—An introduction. *Energy Policy*, *41*, iii–xiv. https://doi.org/10.1016/j.enpol.2011.12.033

American Bureau of Shipping (ABS). (2019). "Setting the Course to Low Carbon Shipping – Pathways to Sustainable Shipping." June 2019. https://absinfo.eagle.org/acton/media/16130/setting-the-course-to-low-carbon-shipping-pathways-to-sustainable-shipping-outlook-ii-low

Argus. (2021). *Marine Fuels Prices* [Data file]. https://www.argusmedia.com/
Aronietis, R., Sys, C., van Hassel, E., & Vanelslander, T. (2017). Investigating the bunkering choice determinants: The case of the port of Antwerp. *Journal of Shipping and Trade*, *2*(8), 1–13. https://doi.org/10.1186/s41072-017-0025-7
Autoridad Maritima de Panama. (2021). *Estadisticas* [Data file]. https://amp.gob.pa/estadistica/
Avelino, A. F. T., Baylis, K., & Honey-Roses, J. (2016). Goldilocks and the Raster Grid: Selecting Scale when Evaluating Conservation Programs. *PLoS One*, *11*(12). https://doi.org/10.1371/journal.pone.0167945

Badgett, A., Newes, E., & Milbrandt, A. (2019). Economic analysis of wet waste-to-energy resources in the United States. Energy, 176, 224-234.

Beuthe, M., Jourquin, B., Geerts, J.-F., & Ndjang'Ha, C. K. (2001). Freight transportation demand elasticities: A geographic multimodal transportation network analysis. *Transportation Research Part E: Logistics and Transportation Review*, *37*(4), 253–266. https://doi.org/10.1016/S1366-5545(00)00022-3

Concawe Factsheet. Marine Fuel Facts (2017). Boulevard du Souverain 165, B-1160 Brussels, Belgium. https://www.concawe.eu/wp-content/uploads/2017/01/marine_factsheet_web.pdf

Comer, B., Olmer, N., Mao, X., Roy, B., Rutherford, D. (2017). Black Carbon Emissions and Fuel Use in Global Shipping 2015. International Council on Clean Shipping.

Davis, S., et al. Net Zero Energy Emissions (2018) Science 360: 6396
Dieler, J., Jus, D., & Zimmer, M. (2015). *Fill'er up! Anticipation and Inventory Effects on Fuel Demand* [CESifo].

Dunn, J., Newes, E., Cai, H., Zhang, Y., Brooker, A., Ou, L., Mundt, N., Bhatt, A., Peterson, S., Biddy, M. (2020). Energy, Economic, and Environmental Benefits Assessment of Co-Optimized Engines and Bio-Blendstocks. *Energy Environ. Sci.* 10.1039.D0EE00716A. https://doi.org/10.1039/D0EE00716A.

EPA (2021). Anaerobic Digestion Facilities Processing Food Waste in the United States(2017 & 2018). https://www.epa.gov/sites/default/files/2021-02/documents/2021_final_ad_report_feb_2_with_links.pdf

French, R., Iisa, K., Orton, K., Griffin, M., Christensen, E., Black, S., Brown, K., Palmer, S., Schaidle, J., Mukarakate, C., Foust, T. (2021). Optimizing process conditions during Catalytic

Fast Pyrolysis of pine with Pt/TiO2—improving the viability of a multiple-fixed-bed configuration, *ACS Sust. Chem. Eng.*, 9, 1235–1245, https://doi.org/10.1021/acssuschemeng.0c07025

Garaniya, V., McWilliam, D., Goldsworthy, L., (2011). Chemical Characterization of Heavy Fuel Oil for Combustion Modeling. Proceedings of the World Engineers.

Gawrys, K., Kilpatrick, P. (2004). Asphaltene Aggregation: Techniques for Analysis. Instrument Science & Technology 32(3); 247-253.

Griffin, M., Iisa, K., Wang, H., Dutta, A., Orton, K., French, R., Santosa,D., Wilson, N., Christensen, E., Nash, C., Van Allsburg, K., Baddour, F., Ruddy, D., Mukarakate, C., Schaidle, J. Driving towards cost-competitive biofuels through catalytic fast pyrolysis by rethinking catalyst selection and reactor configuration. *Energy & Environ. Sci.*, 2018, 11, 2904-2918.

Halff, A., Younes, L., & Boersma, T. (2019). The likely implications of the new IMO standards on the shipping industry. *Energy Policy*, *126*, 277–286. https://doi.org/10.1016/j.enpol.2018.11.033

Harris, C. (2012). *Senate Bill 1243 (Lowenthal) Regarding Bunker Fuel*. State Legislation Committee. http://www.longbeach.gov/globalassets/city-manager/media-library/documents/government-affairs/state-resolutions/2012/bunker-fuel_070312-r-21sratt1

Iisa, K., French, R., Orton, K., Dutta, A., Schaidle, J. (2017). Production of Low-Oxygen Bio-Oil via Ex Situ Catalytic Fast Pyrolysis and Hydrotreating, *Fuel,* 207, 413–422. http://dx.doi.org/10.1016/j.fuel.2017.06.098

Hofko, B., Eberhardsteiner, L., Fu, J., Grothe, H., Handle, F., Hospodka, M., Grossegger, D., Nahar, S., Schmets, A., Scarpas, A. (2013). Impact of Maltene and Asphaltene Fraction on Mechanical Behavior and Microstructure of Bitumen. Materials and Structures 49; 829-841.

Humbird, D., Davis, R., Tao, L. et al. (2011). "Process Design and Economics for Biochemical Conversion of Lignocellulosic Biomass to Ethanol: Dilute-Acid Pretreatment and Enzymatic Hydrolysis of Corn Stover." NREL/TP-5100-47764, 1013269. https://doi.org/10.2172/1013269.

IEA (2021), *World Energy Model*, IEA, Paris https://www.iea.org/reports/world-energy-model

International Monetary Fund. (2019). *Market-Based Instruments for International Aviation and Shipping as a Source of Climate Finance* (p. 66). International Monetary Fund.

International Monetary Fund. (2021). *Global price of Brent Crude* [Data file]. https://fred.stlouisfed.org/series/POILBREUSDM

International Maritime Organization (2018). Initial IMO Strategy on Reduction of GHG Emissions from Ships

International Maritime Organization (2019). Amendments to the Annex of the Protocol of 1997 to Amend the International Convention for the Prevention of Pollution from Ships, 1973, as Modified by the Protocol of 1978 Relating Thereto

Jun, W., John, O., You, L., (2013). Understanding Asphaltenes Stability in Marine Fuel Oil Through Separability Number. Information Technology Journal 12; 8510-8513.

Kass, M., Abdullah, Z., Biddy, M., Drennan, C., Hawkins, T., Jones, S., Holladay, J., Longman, D., Newes, E., Theiss, T., Thompson, T., Wang, M. (2018). Understanding the Opportunities of Biofuels for Marine Shipping. ORNL Report No. ORNL/TM-2018/1080. Oak Ridge National Laboratory, Oak Ridge TN.
Keen, M., Parry, I., & Strand, J. (2013). Planes, ships and taxes: Charging for international aviation and maritime emissions. *Economic Policy*, *28*(76), 701–749. https://doi.org/10.1111/1468-0327.12019
Lee, C.-Y., Lee, H. L., & Zhang, J. (2015). The impact of slow ocean steaming on delivery reliability and fuel consumption. *Transportation Research Part E*, *76*, 176–190. https://doi.org/10.1016/j.tre.2015.02.004

McKay, J., Amend, P., Cogswell, T., Harnsberger, P., Erickson, R., Latham, D. (1978). In Petroleum Asphaltenes: Chemistry and Composition, Energy Research and Development Administration, Analytical Chemistry of Liquid Fuel Sources. Advanced in Chemistry. American Chemical Society. Washington DC.
Maritime and Port Authority of Singapore. (2021). *Port Statistics* [Data file]. https://www.mpa.gov.sg/web/portal/home/maritime-singapore/port-statistics
Mazraati, M. (2011). Challenges and prospects of international marine bunker fuels demand. *OPEC Energy Review*, *35*(1), 1–26. https://doi.org/10.1111/j.1753-0237.2010.00182.x

MEPC72, (2018). I. Resolution MEPC. 304 (72). *Initial IMO Strategy on Reduction of GHG Emissions from Ships*

Michaelowa, A., & Krause, K. (2000). International Maritime Transport and Climate Policy. *Intereconomics*, *35*(3), 127–136.

Mulchandani, A., & Westerhoff, P. (2016). Recovery opportunities for metals and energy from sewage sludges. Bioresource technology, 215, 215-226.

Odey, F., & Lacey, M. (2018). *IMO 2020—Short term implications for the oil market* (p. 10). Schroders.
OECD. (2020). *OECD Library—IEA World Energy Statistics and Balances* [Data file]. http://dx.doi.org/10.1787/enestats-data-en
Oum, T. H. (1979). Derived Demand for Freight Transport and Inter-Modal Competition in Canada. *Journal of Transport Economics and Policy*, *13*(2), 149–168.
Parry, I., Heine, D., Kizzier, K., & Smith, T. (2018). *Carbon Taxation for International Maritime Fuels: Assessing the Options* (IMF Working Paper WP/18/203; p. 39). International Monetary Fund.
Pindyck, R. S., & Rubinfled, D. L. (1991). *Econometric Models and Economic Forecasts*. McGraw-Hill.

Rogel, E., Leon, O., Espidel, Y., Gonzalez, Y. (2001). Asphaltene Stability in Crude Oils. Society of Petroleum Engineers 16.

Rogers, J., Stokes, B., Dunn, J., Cai, H., Wu, M., Haq, Z., Baumes, H. (2017). An Assessment of the Potential Products and Economic and Environmental Impacts Resulting from a Billion Ton Bioeconomy. *Biofuels, Bioprod. Bioref. 11* (1), 110–128. https://doi.org/10.1002/bbb.1728.
Saad, M. M., Austen, S., & Taylor, S. (1985). Demand for Australia's International Sea Freight Task. *Forum Papers of the 10th Australian Transport Research Forum*, *2*, 71–92.

Seiple, T. E., Skaggs, R. L., Fillmore, L., & Coleman, A. M. (2020). Municipal wastewater sludge as a renewable, cost-effective feedstock for transportation biofuels using hydrothermal liquefaction. Journal of Environmental Management, 270, 110852.

Smith, K., Gaston, K. (2019). NREL 2.4.1.301 FY19 Q3 Milestone: Enable coupled reactor + catalytic fast pyrolysis kinetic model verification at scale, NREL

Smith, T., Raucci, C., Haji Hosseinloo, S., Rojon, I., Calleya, J., Suarez De La Fuente, S., Wu, P., & Palmer, K. (2016). *CO2 emissions from international shipping: Possible reduction targets and their associated pathways* (p. 61). UMAS.
State of Washington. (2021). *Vessel to Vessel Oil Transfer*. Department of Ecology.
Stock, J. H., & Yogo, M. (2010). Testing for Weak Instruments in Linear IV Regression. In *Identification and Inference for Econometric Models* (pp. 80–108). Cambridge University Press.

Tattini, J., J. Teter. (2020). *International Shipping*, International Energy Association, Paris https://www.iea.org/reports/international-shipping

The Northwest Seaport Alliance. (2021). *Cargo Statistics* [Data file]. https://www.nwseaportalliance.com/about-us/cargo-statistics
UNCTAD. (2020). *UNCTAD Stat—Maritime Transport* [Data file]. https://unctadstat.unctad.org/wds/ReportFolders/reportFolders.aspx
U.S. Environmental Protection Agency. (2008). *Global Trade and Fuels Assessment—Future Trends and Effects of Requiring Clean Fuels in the Marine Sector* (No. EPA420-R-08–021; p. 197). U.S. Environmental Protection Agency.

U.S. Energy Information Administration (EIA) (2019). "More stringent marine sulfur limits mean changes for U.S. refiners and ocean vessels" February 4, 2019. https://www.eia.gov/todayinenergy/detail.php?id=38233

Winebrake, J. J., Green, E. H., Comer, B., Li, C., Froman, S., & Shelby, M. (2015a). Fuel price elasticities for single-unit truck operations in the United States. *Transportation Research Part D*, *38*, 178–187. https://doi.org/10.1016/j.trd.2015.05.003

Winebrake, J. J., Green, E. H., Comer, B., Li, C., Froman, S., & Shelby, M. (2015b). Fuel price elasticities in the U.S. combination trucking sector. *Transportation Research Part D*, *38*, 166–177. https://doi.org/10.1016/j.trd.2015.04.006

APPENDIX A. BASELINE FUEL DATA SOURCE, ASSUMPTIONS, AND CALCULATIONS SUPPORTING SUPPLY AND DEMAND ECONOMICS

The price data in this appendix were used to determine the supply and demand curve results presented in Section 1. The results in Table A.1 correspond to the results shown in Figure 1. Specifically, an augmented Dickey–Fuller test was performed on each variable to check for non-stationarity of the time series; the null hypothesis of a unit-root process could not be rejected for any of the variables. A first-order differentiation resolved the non-stationarity issue, so the model was computed in first differences. Monthly dummy variables were added to account for seasonality in the time series.

Table A.1. Summary statistics

Region	Variable	Freq.	N	Mean	Std. dev.	Min	Max
World	HSFO sales	A	29	145,639	31,186	94,438	184,052
	Containers	A	29	382,273	232,638	85,597	795,736
	HSFO price	A	29	266	192	66	665
	Oil price	A	29	49	33	13	112
Singapore	HSFO sales	M	300	2,452	1,028	972	4,379
	Containers	M	300	2,056	670	867	3,268
	HSFO price	M	300	305	191	55	742
	Oil price	M	300	55	33	10	134
Panama	HSFO sales	M	84	245	51	142	362
	Containers	M	84	233	32	178	322
	HSFO price	M	84	393	143	133	646
	Oil price	M	84	71	24	31	116
Seattle–Tacoma	HSFO sales	M	108	98	19	56	146
	Containers	M	108	300	28	221	374
	HSFO price	M	108	459	161	157	740
	Oil price	M	108	80	27	31	125

Tabulated Results

The results of the first and second stages of the two-stage least squares model are shown in Table A.2. The first stage confirms the applicability of crude oil prices as an instrument for bunker fuel prices, and the results for the Stock and Yogo (2010) method reject the null hypothesis of weak instruments.

Table A.2. Two-stage least squares estimates by region

	World	Singapore	Panama	Seattle–Tacoma
First stage				
Oil price	1.014 [0.076]***	0.812 [0.045]***	1.005 [0.082]***	0.739 [0.066]***
Time dummies	No	Yes	Yes	Yes
R-squared	0.913	0.615	0.708	0.585
Stock and Yogo test	218.61 (16.38)	389.02 (16.38)	143.68 (16.38)	130.49 (16.38)
Second stage				
HSFO price	0.043 [0.032]	−0.142 [0.060]**	−0.267 [0.174]	0.321 [0.391]
Containers	0.456 [0.148]***	0.145 [0.142]	−0.019 [0.121]	0.694 [0.308]**
Lag HSFO sales	−0.051 [0.161]	−0.260 [0.061]***	−0.236 [0.114]**	−0.448 [0.092]***
Constant	−0.015 [0.014]	0.032 [0.015]**	0.092 [0.051]*	0.145 [0.083]*
Time dummies	No	Yes	Yes	Yes
Frequency	Annual	Monthly	Monthly	Monthly
Observations	28	299	83	107
R-squared	0.408	0.267	0.181	0.219

Notes: The dependent variable is log fuel oil demand. Significance levels: *** 1%, ** 5%, * 10%. Standard deviations shown in brackets. Stock and Yogo test: Cragg–Donald statistic; critical values shown in parentheses.

At the global level, port activity showed a significant and positive effect on fuel demand, as expected, but own-price elasticity was not significant. A possible explanation for the elasticity might be a measurement error regarding global bunker fuel sales. As noted by the US Environmental Protection Agency (2008), world data on marine fuel demand varies considerably across sources. Marine fuels are usually not properly accounted for in domestic oil demand statistics because of incomplete port reporting and because fuels are consumed at sea. Therefore, different modeling approaches are used to estimate their demand, with large discrepancies between organizations (Halff et al., 2019; Mazraati, 2011). Another explanation for an insignificant own price elasticity is the spatial aggregation and frequency of the data, which might be masking the effects of port competition. This modifiable areal unit problem can bias the estimates toward zero because the model is estimated at a different scale from the data generating process (Avelino et al., 2016).

At finer geographical and temporal scales, the results indicate a significant negative own-price elasticity of −0.14 for the Port of Singapore. This result is consistent with the previous literature (ranging from −0.45 to −0.01) and shows that demand has low sensitivity to price changes, further confirming that marine transport is the most competitive long-distance mode and thus can effectively absorb price fluctuations. However, estimated own-price elasticities were not significant for Panama or the Port of Seattle–Tacoma.

APPENDIX B. DETAILS OF VARIABLES AND ASSUMPTIONS USED TO DETERMINE THE TECHNOECONOMICS OF HTL OILS

As stated in Section 2, researchers at PNNL conducted preliminary analysis on three feedstock HTL conversions with different hydrotreating strategies (no hydrotreating, partially hydrotreating, and fully hydrotreating). The feedstocks included sludge HTL, sludge/FW/FOG HTL, and sludge/FOG. Figure B.1 shows the MFSP results against the 2020 SOT [1]. A key feature of this analysis is the assumption of a large HTL plant at scale of 1,000 dry metric ton/day (tpd) combined with an upgrading plant in one regional waste resources hub. Feedstock cost is assumed to be negligible. Also, this analysis includes a 2022 projection on hydrotreating catalyst life and weight hourly space velocity.

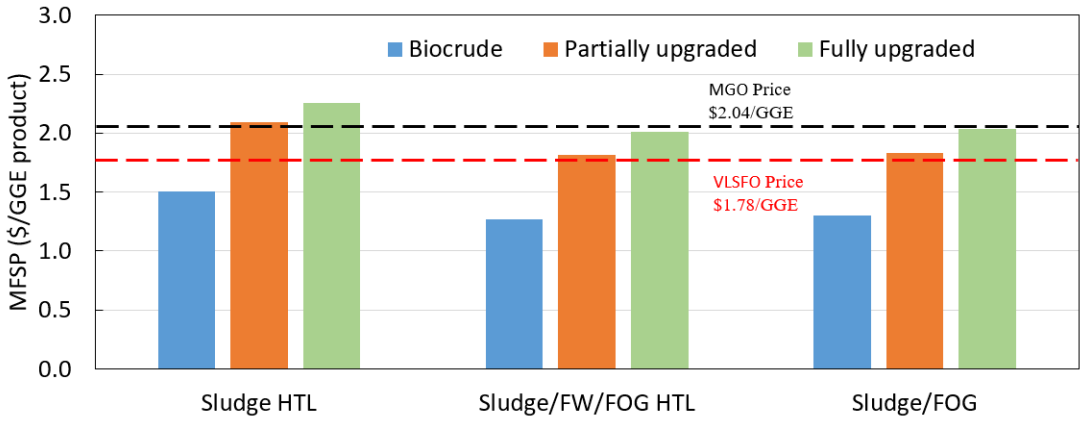

Figure B.1. Modeled MFSP for three feedstocks under different hydrotreating strategies for marine fuel application. (MGO and VLSFO price is based on the reported price in 2021)

Process Model and Assumptions

The PNNL marine biofuels team leveraged the HTL runs of wet waste such as sludge, FW, FOG waste, and manure to identify opportunities of converting wet waste to marine fuels. The analysis has included the sludge HTL from the Detroit wastewater treatment plant (Great Lakes Water Authority), sludge/food/FOG waste blend, and sludge/FOG waste blend. Plant scale is a key economic driver for this pathway, as shown in the sludge HTL design case [2]. Preliminary wet waste resource analysis shows that 82% of the total wet waste resource in the United States could be collected at sites over a 1,000 tpd scale at a transportation cost of $50/MT (based on 2014 transportation costs) [3]. To take advantage of economies of scale, a large HTL plant at a scale of 1,000 tpd is modeled and evaluated. Another strategy to reduce cost is to minimize the number of processing steps by eliminating the hydrocracker unit and simplifying the hydrotreating steps since the raw or mildly hydrotreated biocrude could be blended with existing maritime fuels. The hydrotreating equipment includes a guard bed for metals and mild heteroatom removal and a main hydrotreating reactor for removing oxygen, nitrogen, and sulfur to the extent possible. Different hydrotreating steps could be required for HTL biocrude from different wet wastes because of the variability of feedstock compositions. Figure B.2 shows the process configuration used for this pathway, as well as the potential minimum processing requirements for marine fuel blendstocks. The waste HTL processing plant is sited at the wastewater treatment plant. Biocrude upgrading is also colocated with the HTL plant in this scenario (i.e., no transportation cost for biocrude). Table B.1 summarizes the key process technical assumptions associated with HTL of different feedstocks.

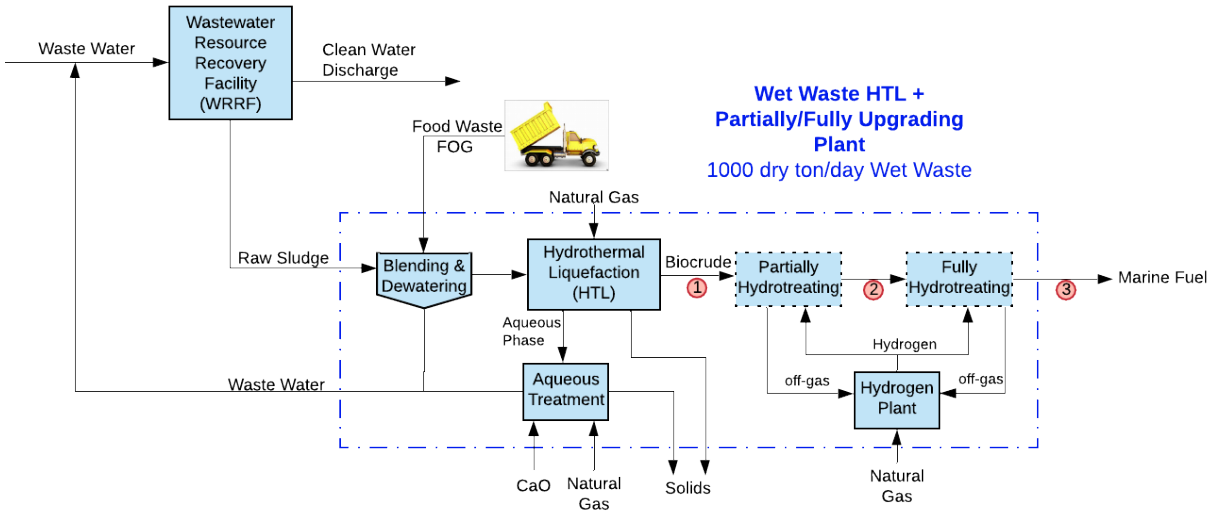

Figure B.2. The potential sampling locations for the biocrude/bio-oil for marine fuel analysis.

Table B.1. Key assumptions for HTL conversion with three feedstocks

	Sludge HTL	Sludge/food/FOG HTL	Sludge/FOG HTL
HTL scale (tpd)	1,000	1,000	1,000
Upgrader scale (mmgal/year biocrude)	31	34	36
Feedstock composition	50/50 primary/secondary Sludge (Great Lakes Water Authority)	50/40/10 Sludge/FW/FOG	80/20 Sludge/FOG
Feed solid (wt %)	20	25	17
Ash-free solid (wt %)	15	21	17
Biocrude yield from testing	44	46	50
Transportation cost of waste feedstock to HTL ($/dry ton waste)	45.36 (100 mi radius)	45.36 (100 mi radius)	45.36 (100 mi radius)
Transportation cost of biocrude ($/GGE)	0 (colocated with HTL)	0 (colocated with HTL)	0 (colocated with HTL)
Hydrotreating catalyst life (year)	1.0	1.0	1.0
H_2 consumption in guard bed (g/g dry feed)	0.027[a]	0.027[a]	0.027[a]
H_2 consumption in main bed (g/g dry feed)	0.019	0.022[b]	0.024

[a] The average H_2 consumption in the guard bed is based on the data with a H_2 consumption range of 0.007 to 0.035 g/g dry feed for algae HTL at different hydrotreating conditions.
[b] Based on sludge HTL and sludge/FOG HTL operating data; the results will be updated once the hydrotreating data is available.

Economic Analysis

The modeled costs are based on a set of *n*th plant financing and operating assumptions used for all of BETO's conversion pathway TEAs. The MFSP was determined from the discount cash flow rate of return

analysis, and all costs are in 2016 US dollars. Table B.2 lists the modeled biocrude MFSP from sludge HTL, sludge/food/FOG HTL and sludge/FOG HTL. Biocrudes derived from sludge/food/FOG and sludge/FOG have a similar MFSP of approximately $1.30/GGE, whereas biocrude from sludge HTL has a relatively higher MFSP of $1.51/GGE. All of the modeled biocrude MFSPs are lower than the reported VLSFO price ($1.78/GGE). These results show that feedstock type has enormous influence on the processing costs. This effect is attributed to variation in feedstock composition (e.g., lipid, protein, and carbohydrate) and HTL operating conditions such as feed solid content. Biocrude yield is a significant economic driver since high lipid content will increase the biocrude yield, and high levels of solid matter in the feedstock will reduce capital costs of the HTL reactor.

Table B.2. Economic summary of HTL biocrude of three feedstocks

Parameter	Sludge HTL	50% sludge/40% food/10% FOG HTL	80% sludge/20% FOG HTL
Avoided disposal credits ($/dmtu)	200	107	50
Transportation cost ($/dmtu)	50	50	50
Biocrude MFSP without potential credits ($/GGE)	1.51	1.27	1.30
Biocrude MFSP with potential credits ($/GGE)	0.18	0.78	1.30
Biocrude MFSP contribution ($/GGE)			
Feedstock potential credits	1.33	0.49	0.00
Operating cost	0.71	0.57	0.56
Capital cost and taxes	0.80	0.70	0.74
Feed solids (wt %)			
Ash included	20	25	17
Ash-free	15	21	17
Biocrude yield: dry, ash-free (wt %)	44	46	50
Biocrude production (mmGGE/year)	31.2	33.8	35.8
Total installed equipment cost ($MM)	105	96	108
Total capital investment ($MM)	210	192	215

This analysis does not consider the potential avoided disposal costs for the wet waste. For example, the sludge management and disposal costs account for about 40%–65% of the total wastewater treatment plant's operating expenses. The common routes of sludge management include land application, landfill-based disposal, and incineration. The solids reduction resulting from the HTL process would conceivably result in significant savings in avoided disposal costs to the plant. In fact, the numerous sources indicate a wide range of the sludge disposal credits ($200–$800/dry ton) depending on the management practice, location and policy, and so on (Seiple et al. 2020; Mulchandani et al. 2016).

A recent national analysis shows that national sludge weighted price is around $200/dmtu and FOG price is around $551/dmtu (Badgett et al. 2019). For a conservative analysis, $200/dmtu sludge can be used as an avoided disposal cost. However, even though waste disposal costs are lowered, paying out an average tipping fee is still required. In this study, the average tipping fee ($157/dmtu) paid to the FW anaerobic digestion plants in a recent EPA report was used (EPA 2021). With reductions in wet waste price and potential transportation cost, the MFSPs for the three feedstock scenarios could be lower as shown in Table B.2.

Table B.3 lists the biocrude properties from sludge HTL, sludge/food/FOG HTL, and sludge/FOG HTL. Biocrude derived from sludge/FOG HTL has the lowest sulfur content, 0.3 wt %, whereas the other two biocrudes' sulfur contents are relatively high.

Table B.3. Biocrude properties of three feedstocks

Operating conditions and results	Sludge HTL	Sludge/food/FOG HTL	Sludge/FOG HTL
HTL dry biocrude analysis (wt %)			
Carbon	78.5	76.1	77.9
Hydrogen	10.7	10.5	10.9
Oxygen	4.7	8.6	7.2
Nitrogen	4.8	4.2	3.6
Sulfur	1.2	0.7	0.3
Ash	0.06	0.0	0.05
HTL dry biocrude hydrogen:carbon ratio	1.6	1.6	1.7
HTL biocrude dry higher heating value (Btu/lb) (MJ/kg in parentheses)	16,900 (39.5)	16,700 (38.9)	16,900 (39.3)
HTL biocrude moisture (wt %)	4.4	4.6	3.2
HTL biocrude wet density at 25°C (g/ml)	0.98	0.96	0.95

Table B.4 lists the modeled MFSPs of partially and fully hydrotreated fuel from three feedstocks and their cost allocations. As expected, fully upgraded fuel MFSPs are higher than the partially upgraded fuel MFSPs because of the higher hydrogen consumption. As shown in Table B.4, producing fully upgrading fuel increased the modeled MFSP by $0.19/GGE on average for the three feedstocks. Additionally, feedstock cost is the largest contributor to the MFSP of partially and fully upgraded fuel.

Table B.4. Economic summary of partially and fully hydrotreated fuel from three feedstocks

Parameter	Sludge HTL		Sludge/food/FOG HTL		Sludge/FOG HTL	
	Partially	Fully	Partially	Fully	Partially	Fully
MFSP ($/GGE)	2.09	2.25	1.81	2.01	1.83	2.04
MFSP contribution ($/GGE)						
Feedstock cost	1.61	1.63	1.34	1.37	1.37	1.40
Operating cost	0.24	0.29	0.24	0.30	0.23	0.30
Capital cost and taxes	0.24	0.33	0.23	0.34	0.23	0.34
Total installed equipment cost ($MM)	35	49	35	50	37	53
Total capital investment ($MM)	70	97	70	100	74	106

APPENDIX C. BIO-OIL TEA

Bio-Oil and Other Biofuel Pathway and TEA Findings

This section summarizes the analysis performed to identify opportunities for conversion pathways aligned with the objectives mentioned previously, with the specific conversion routes as follows. The TEA results are summarized in Figure C.1. Detailed descriptions for each pathway are provided in Sections 2–4.

- Pathway 1: Ex situ CFP with vapor phase upgrading over a Pt/TiO_2 catalyst and with whole bio-oil and lighter cuts removed. This pathway also includes a 2030 projection on increase yield of the bio-oil product
- Pathway 2: Ex situ CFP with vapor phase upgrading over a ZSM-5 catalyst and with whole bio-oil and lighter cuts removed
- Pathway 3: LFG to steam methane reforming followed by fuel production via FT synthesis to hydrocarbon blendstocks
- Pathway 4: LEO from the lignocellulosic ethanol biorefinery and standalone LEO plant

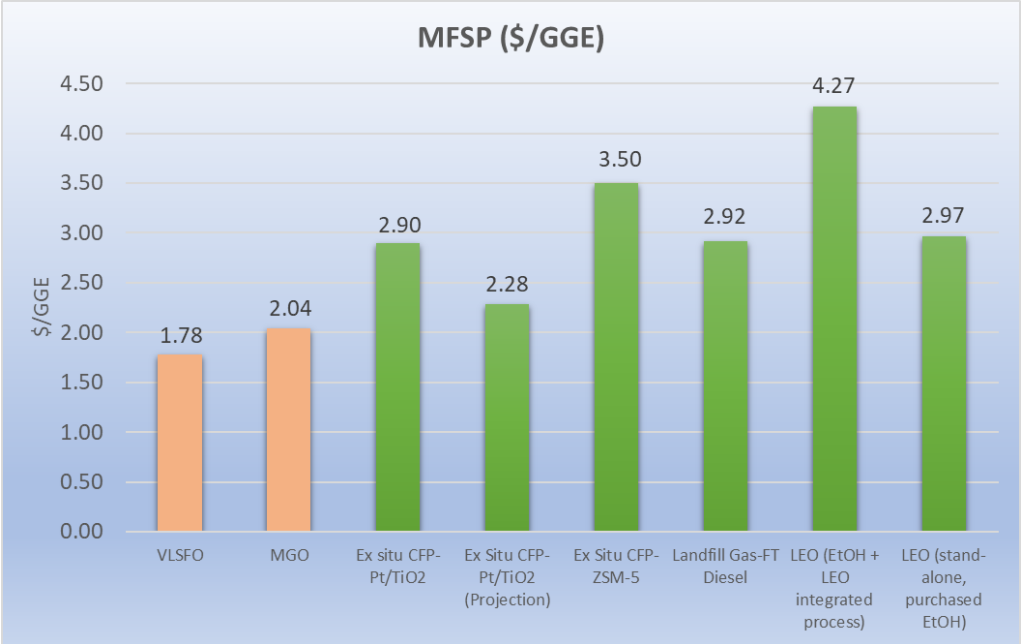

Figure C.1. TEA summary ($/GGE). For each ex situ CFP pathway, the corresponding MFSPs for whole oil and lighter cuts are identical because the MFSPs were determined based on the total fuel energy produced.

Pathway 1: Ex situ CFP with vapor phase upgrading over a Pt/TiO_2 catalyst with whole bio-oil and lighter cuts removed

This pathway also includes a 2030 projection on increase yield of the bio-oil product. The simplified process flow diagram for Pathway 1 is shown in Figure C.2.

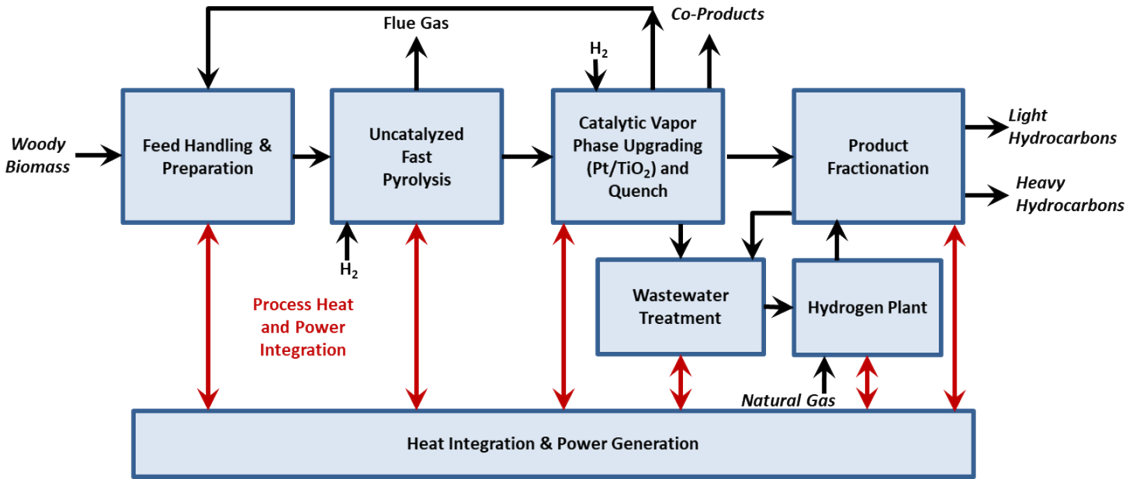

Figure C.2. Main process steps for Pathway 1.

A 50/50 blend of forest residues and clean pine were used for the TEA models. All plants are based on a 2,000 MT/day feedstock rate (Figure C.2). The process model for uncatalyzed fast pyrolysis uses a circulating fluidized bed design. The dual-bed reactor system includes a riser reactor for fast pyrolysis and a char combustor to heat circulating sand to provide the reaction temperatures at 500°C. The solids are removed via cyclones and a hot gas filter. The hot gas filter is required to prevent plugging of the fixed bed ex situ catalytic vapor upgrading reactor with Pt/TiO_2 with 0.5 wt % Pt loading. The ex situ reactor was maintained at 400°C with a biomass to catalyst ratio of 12. The reactor configurations are shown in Figure C.3 [1].

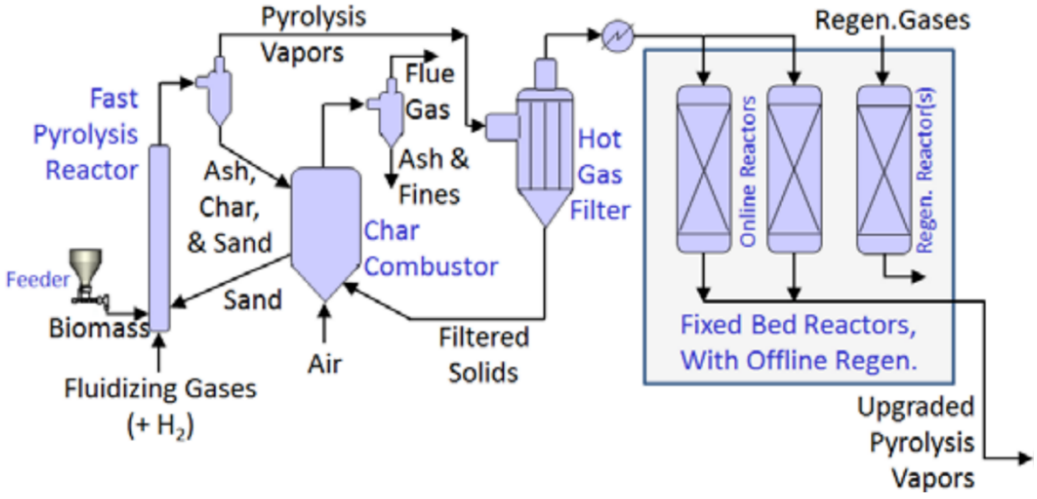

Figure C.3. Fast pyrolysis and vapor phase upgrading with Pt/TiO_2.

After vapor phase upgrading via the catalyst reactor, the vapors are cooled via an indirect heat exchanger to the dew point of the vapor stream. The heavy organic bio-oil is condensed in an absorber/condenser with product from a downstream condenser used as the quench liquid. The uncondensed vapors from the first absorber/condenser are sent through another set of heat exchangers before entering a second absorber/condenser column for a final quench. The bottom product from the second condenser is separated into an aqueous stream and sent to the wastewater treatment.

For the whole-oil pathway, the heavy hydrocarbon stream from the first condenser and the light hydrocarbon stream from the second condenser are combined. For the pathway with the lighter cuts removed, the product streams are kept separate and sold as two distinct products.

For the case involving the Pt/TiO_2 catalyst, light oxygenates were recovered from the gaseous stream of the second condenser. The oxygenate stream was sent to an adsorption system to remove the light oxygenates, and the stream was sent through a series of distillation columns to recover acetone and MEK as saleable products.

The overall yield on a mass basis (mass bio-oil/mass biomass feedstock) for the base Pt/TiO_2 case is 23%, with the 2030 projection case being 31%.

A process flow diagram of the product fractionation is show in Figure C.4.

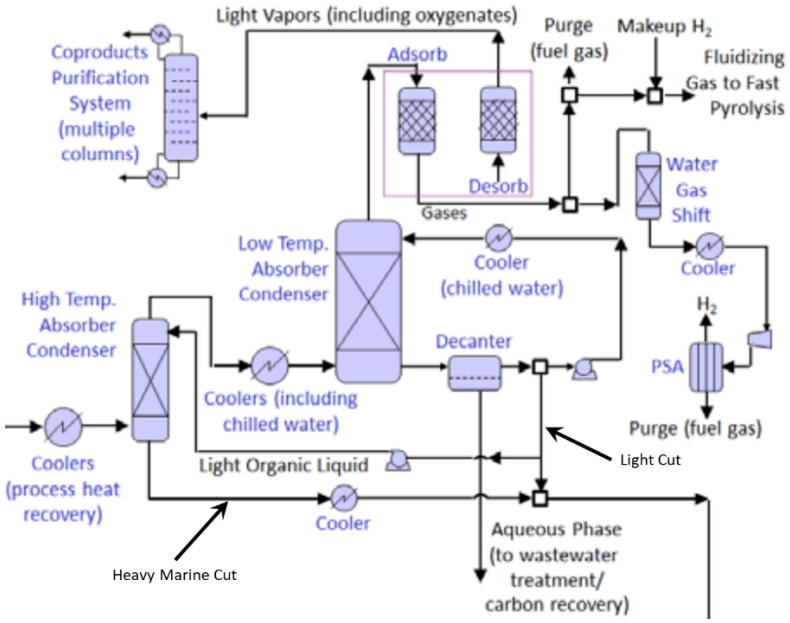

Figure C.4. Process block diagram for product fractionation.

Pathway 2: Ex situ CFP vapor phase upgrading over a ZSM-5 catalyst with whole bio-oil and lighter cuts removed

The simplified block diagram for Pathway 2 is shown in Figure C.5. Pathway 2 represents a similar configuration to Pathway 1 expect for the use of a fluidized-bed reactor with ZSM-5 impregnated catalyst and the lack of a hot gas filter entering the vapor upgrading step. The hot vapor stream exiting the uncatalyzed fast pyrolysis reactor is sent directly to upgrading without filtration. The hot vapors enter the fluidized bed that uses a ZSM-5 catalyst.

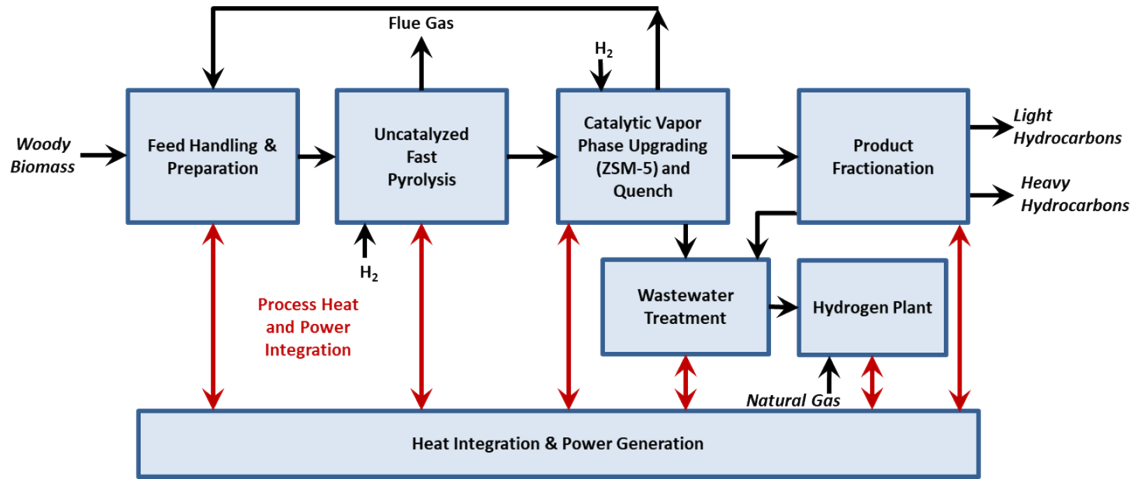

Figure C.5. Main process steps for Pathway 2.

As with the Pt/TiO_2 case, the vapors enter the catalytic upgrading step at 500°C. The hot vapors enter the ex situ riser reactor with regenerated ZSM-5 catalyst. The upgraded vapors leave the riser reactor, and any solids and spent catalyst are removed via cyclone. The spent catalyst is sent to a regeneration reactor that uses air and reaction cases to burn off any coke or char from the reactor. The vapors from the catalyst regenerator and sent through a cycle to remove any spent char or ash. The flue gases from the regenerator are used in the process for hydrogen and steam generation. All three reaction systems in the ex situ ZSM-5 case are operated at the same condition of 500°C. Because of the nature of the products produced from the ZSM-5 catalyst, no coproduct in the form of acetone or MEK is produced. The reactor configurations for the ZSM-5 catalyst case are show in Figure C.6. Again, for the whole-oil production, the light and heavy hydrocarbon streams are combined, whereas for the heavier cuts, the two hydrocarbon streams remain separate.

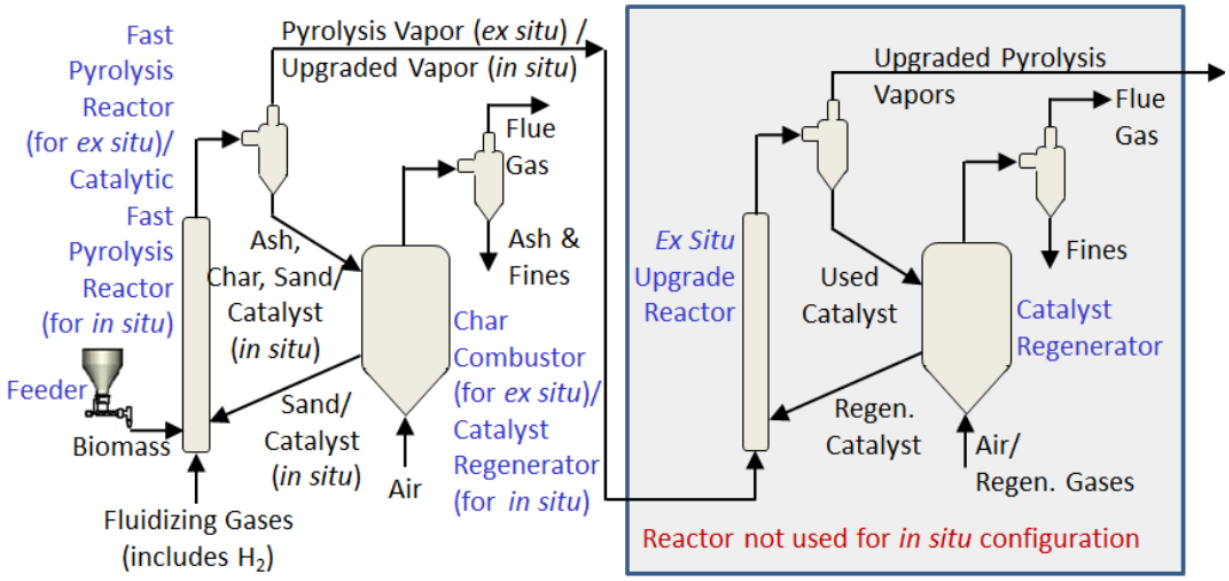

Figure C.6. Fast pyrolysis and vapor phase upgrading with ZSM-5.

The process downstream of the fast pyrolysis reactor and vapor phase upgrading is the same as in the Pt/TiO_2 case.

Ex situ CFP TEA summary

The TEA results are presented in Table C.1. The modeled costs are based on a set of *n*th plant financing and operating assumptions used for all of BETO's conversion pathway TEAs. Based on these assumptions, the MFSPs obtained from the discount cash flow rate of return analysis for the three pathways increase in the order of \$2.28/GGE for Pt/TiO_2 in the 2030 projection, \$2.90/GGE for Pt/TiO_2, and then \$3.50/GGE for ZSM-5.

Table C.1. Economic summary for natural gas and LFG pathways to FT fuels

Parameter	1: Fixed Bed Pt/TiO2	1: Fixed Bed Pt/TiO2 - 2030 projection	2: Fluidized Bed ZSM-5
MFSP, \$/GGE	\$2.90	\$2.28	\$3.50
MFSP Contributions:			
Feedstock Costs, \$/GGE	\$1.22	\$0.92	\$1.12
Operating Costs & Credits, \$/GGE	\$0.23	\$0.16	\$0.82
Capital Charges & Taxes, \$/GGE	\$1.45	\$1.21	\$1.56
Total Bio-oil Production, MM GGE/yr	41.2	55.1	45.2
Light Bio-Oil Product, MMGGE/yr	21.6	26.0	26.7
Heavy Bio-Oil Product, MMGGE/yr	19.7	29.2	18.5
Product Yield (wt biomass feedstock/wt bio-oil)	23.8%	31.3%	22.1%
Total Installed Equipment Cost (TIC), \$MM	\$281	\$273	\$296
Total Capital Investment (TCI) \$MM	\$522	\$507	\$548

Lower MFSP for the Pathway 1 2030 projection is attributed to its higher yield compared with the state of the technology case (55.1 vs. 41.2 mmGGE/year, or 33.7% higher). Pathway 3 has the highest MFSP because it has the lowest process conversion efficiency and highest capital costs compared with the other CFP pathways.

The product distribution between light and heavy bio-oil is similar with a roughly 45%/55% split for the light cuts and heavy cuts, respectively, for the Pt/TiO_2 case. Because of the different product distribution produced over the ZSM-5 catalyst, the light vs. heavy cut is approximately a 60%/40% split.

Table C.2 represents the main product distribution, fuel yields, and other process consumables.

Table C.2. Product distributions, consumables, and air emissions for fast pyrolysis pathways

	Production Rate								
	Pt/TiO2			Pt/TiO2 - 2030 projection			ZSM-5		
Products	**lb/h**	**GGE (LHV)/h**	**MMBtu/h (LHV**	lb/h	GGE (LHV)/h	MMBtu/h (LHV)	lb/h	GGE (LHV)/h	MBtu/h (LHV)
Light Cut	19,399	2,492	153	25,494	3,291	201	24,354	3,392	192
Heavy Cut	23,614	2,738	186	32,098	3,699	253	16,262	2,344	128
Total (Whole Bio-oil)	43,013	5,230	339	57,593	6,991	454	40,616	5,737	320
By-products									
Excess electricity (kw)	15,160			5,210			20,612		
MEK (lb/hr)	1,186			1,106			-		
Acetone (lb/hr)	5,084			4,987			0		
Biorefinery Resource Consumption	**lb/h**	**lb/GGE**	**lb/MMBtu**	**lb/h**	**lb/GGE**	**lb/MMBtu**	**lb/h**	**lb/GGE**	**lb/MMBtu**
Blended woody biomass (wet)	204,131	39	602	204,131	29	450	204,131	36	637
Blended woody biomass (dry)	183,718	35	542	183,718	26	405	183,718	32	574
Sand makeup	159	0	0	159	0	0	159	0	0
Natural Gas	165	0	0	3,545	1	8	374	0	1
Zeolite catalyst	-	-	-	-	-	-	229	0	1
Fixed-Bed VPU Catalyst (1% Pt/TiO2)	7	0	0	7	0	0	-	-	-
Hydrotreating Catalyst (sulfided CoMo)	-	-	-	-	-	-	-	-	-
Hydrocracking Catalyst (crystalline Si-Al)	-	-	-	-	-	-	-	-	-
ZnO (reforming cleanup)	0	0	0	1	0	0	0	0	0
HDS (reforming cleanup)	0	0	0	0	0	0	0	0	0
Steam Reforming Catalyst	0	0	0	2	0	0	0	0	0
Shift Catalyst	0	0	0	3	0	0	0	0	0
PSA Adsorbent	3	0	0	68	0	0	7	0	0
50 wt% Caustic	232	0	1	232	0	1	232	0	1
Net Water Makeup	52,524	10	155	39,882	6	88	20,678	4	65
Boiler feed water chemicals	2	0	0	2	0	0	2	0	0
Cooling tower chemicals	1	0	0	1	0	0	1	0	0
No. 2 diesel fuel	71	0	0	71	0	0	71	0	0
Waste Streams	**lb/h**	**lb/GGE**	**lb/MMBtu**	lb/h	lb/GGE	lb/MMBtu	lb/h	lb/GGE	lb/MMBtu
Solids purge from fluidized bed reactors	2,064	0	6	2,063	0	5	2,075	0	6
Wastewater	17,464	3	51	16,635	2	37	16,804	3	52
Air Emissions	**lb/h**	**lb/GGE**	**lb/MMBtu**	lb/h	lb/GGE	lb/MMBtu	lb/h	lb/GGE	lb/MMBtu
CO2 (Fossil)	453	17,199	1	9,725	268,275	21	1,025	50,032	3
CO2 (Biogenic)	190,250	36	561	147,495	21	325	218,216	38	681
CH4	-	-	-	-	-	-	-	-	-
CO	-	-	-	-	-	-	-	-	-
NO2	1	0	0	2	0	0	1	0	0
SO2	85	0	0	85	0	0	85	0	0
H2O	123,319	24	364	104,959	15	231	103,410	18	323
H2S	-	-	-	-	-	-	-	-	-
Combustor Feed Stream Heating Values	**% Biogenic**	**LHV (MMBtu/**	**HHV (MMBtu/**	Biogenic C	HV (MMBtu/h)	HV (MMBtu/h)	Biogenic C	HV (MMBtu/h)	HV (MMBtu/h)
Char Combustor	100%	298	308	100%	299	308	100%	251	261
Reformer Fuel Combustor	100%	348	386	89%	207	231	99%	305	337

The Pathway 1 2030 projection uses more natural gas to increase the yield of the product because of an increased need for hydrogen in the vapor phase upgrading step. All pathways supply an excess amount of electricity to the grid from the process off-gases in the fast pyrolysis and hydrogen production processes.

The heating values, densities, and carbon weight percentages of the three CFP pathways are show in Table C.3.

Table C.3. Fuel properties of the CFP pathways

	Pt/TiO2			Pt/TiO2 - 2030 projection			ZSM-5		
	LHV (Btu/gal)	Density g/gal	C (wt%)	LHV (Btu/gal)	Density g/gal	C (wt%)	LHV (Btu/gal)	Density g/gal	C (wt%)
Whole Oil	87,738	3,167	77%	87,579	3,167	77%	101,906	3,167	82%
Light Cut	92,698	3,167	80%	93,148	3,167	80%	100,495	3,167	81%
Heavy Oil	83,650	3,167	88%	83,144	3,167	88%	104,004	3,167	85%

APPENDIX D. FISCHER–TROPSCH PATHWAY AND APPROACH DETAILS

The simplified block diagram for the selected FT process is shown in Figure D.1.

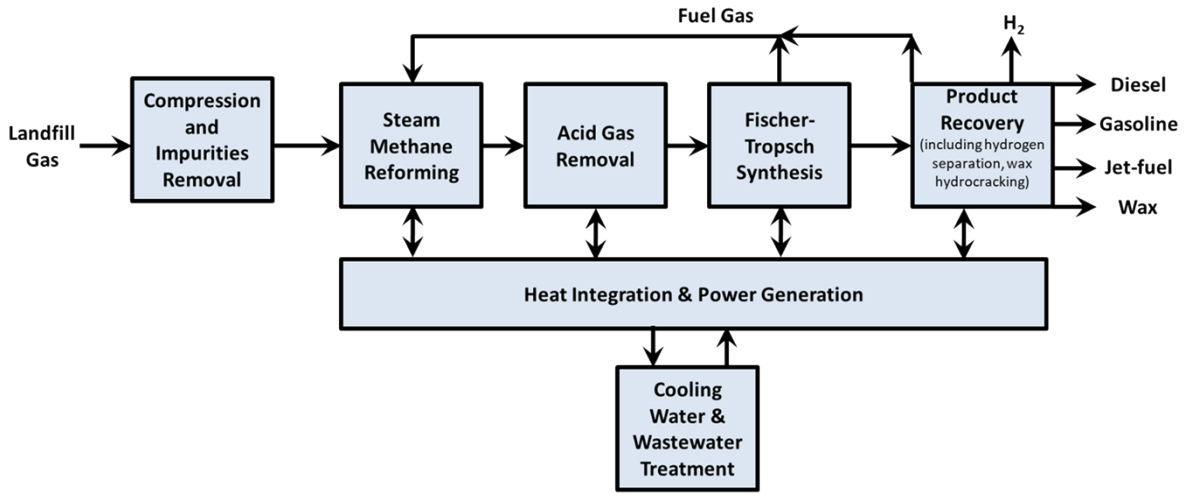

Figure D.1. Main process steps for Pathway 3.

LFG differs in composition from natural gas, with approximately 40 vol % CO_2. A compositional breakdown and comparison with standard natural gas is provided in Table D.1. The pressure of LFG emissions from the landfill is low (~1.6 psig), and it must be compressed before entering the steam methane reformer at 30 psi (2.1 bar). After compression, an iron bed removes the H_2S in the feed stream, followed by an activated carbon bed to remove any remaining siloxanes.

Table D.1. Fuel compositions of LFG and natural gas [3]

	LFG	Natural Gas
Component	**Mole percent (%)**	**Mole percent (%)**
CH_4	57.1	94.4
C_2H_6	0	3.1
C_3H_8	0	0.1
Iso-C_4H_{10}	0	0.5
N-C_4H_{10}	0	0.1
Iso-C_5H_{12}	0	0.2
CO	6 ppm	0
N_2	2.4	1.1
CO_2	40.5	0.5
H_2S	68 ppm	6 ppm
Siloxanes	6 ppm	0

With the steam methane reforming, the primary reaction is to convert methane gas to carbon monoxide and hydrogen.

Steam reforming:

$$CH_4 + H_2O \rightarrow CO + 3H_2$$

Additionally, unconverted syngas from the FT process may be recycled back to the reformer or combusted to provide some or all of the heat necessary for the endothermic reforming reactions.

The syngas stream consisting mostly of CO, H_2, H_2O, and CO_2 is cooled and then compressed to 425 psi (29.3 bar) before entering the acid gas removal system, which removes the bulk of the H_2S and CO_2 from the process gas.

FT synthesis is a catalytic conversion process, which converts the synthesis gas to a mixture of reaction products such as diesel, gasoline, jet fuel, and wax products. The overall reaction involved in the FT synthesis is as follows:

$$(2n + 1)H_2 + nCO \rightarrow C_nH_{2n+2} + nH_2O$$

The FT polymerization process offers the ability to produce liquid hydrocarbon fuels with relatively low sulfur and aromatic content. For this process, the H_2/CO ratio entering the FT reactor was maintained at 1.5:1 by sending a portion of the synthesis gas stream to a pressure swing adsorption system with the off-gas feeding the FT reactor. The effect of the lower H_2/CO ratio results in a less than stoichiometric ratio being fed to the reactor, and thus, only 78% of the CO is consumed in the FT reactor, compared with a typical natural gas feedstock that has an 85% conversion of CO.

The FT products are condensed and separated through a multi-cut distillation column to separate the product streams. The purified H_2 from the pressure swing adsorption system is used for hydrotreating distillation products to yield blendstocks for gasoline, diesel, and jet fuel, or is used for hydrocracking wax. Wax produced from the hydrocracker is sold as a coproduct. Any excess H_2 not consumed for hydrotreating, or hydrocracking, is sold as a coproduct.

The TEA results are presented in Table D.2. The modeled costs are based on a set of *n*th plant financing and operating assumptions used for all of BETO's conversion pathway TEAs. Based on these assumptions, the MFSP obtained from the discount cash flow rate of return analysis, the LFG pathway, is $2.92/GGE.

Table D.2. Economic summary for natural gas and LFG pathways to FT fuels

Parameter	3: SMR and Fischer-Tropsch using landfill biogas
MFSP, $/GGE	$2.92
MFSP Contributions:	
Feedstock Costs, $/GGE	$1.89
Operating Costs & Credits, $/GGE	($0.23)
Capital Charges & Taxes, $/GGE	$1.26
Fuel Production, MM GGE/yr	50.2
Fuel Usage, tons per day	2,805
Total Purchased Equipment Cost (TPEC), $MM	$121.30
Total Installed Equipment Cost (TIC), $MM	$274.10
Total Capital Investment (TCI) $MM	$478.40

Table D.3 represents the main product distribution and fuel yields for the LFG pathway. The yields are approximately 41% lower than compared with similar processes using natural gas because of the lower heating value of the LFG and the high concentration (40%) of CO_2 in the feedstock.

Table D.3. Product distributions and yields for the LFG pathway

Key Process Targets	Pathway 3
Fuel Production (MM GGE/yr):	
Naphtha range	9.74
Jet range	18.90
Diesel range	21.27
Total	**49.91**
Fuel yield (GGE/ton fuel):	
Naphtha range	10.58
Jet range	20.52
Diesel range	23.08
Total	**54.18**

The heating values, densities, and carbon weight percentages of the liquid fuels are show in Table D.4. The table shows that the highest production rates are associated with jet fuel and gasoline. However, significant quantities of diesel are produced, which can be directed toward the marine sector.

Table D.4. Fuel properties of Pathway 3

	Landfill Gas - FT				
Products / Co-products	**lb/hr**	**kg/hr**	**LHV (MMBtu/hr)**	**Density (kg/gal)**	**C wt%**
Diesel	7,600	3,447	143.47	2.987	85.00%
Jet fuel	16,533	7,499	313.15	2.728	84.51%
Gasoline	15,762	7,149	278.34	2.861	77.50%
Wax	4,879	2,213	91.85	2.996	84.92%
Hydrogen	1,376	624	71		
Electricity (kWh/hr)		5,844			

APPENDIX E. APPENDIX E. DETAILED APPROACH AND PROCESSES SUPPORTING THE SUSTAINABILITY ANALYLSES

Updates to Argonne's GREET Marine Module

Several enhancements and developments have been made to Argonne's GREET Marine Module. These include the development of marine ammonia, e-Methanol, e-FT fuel, and HFO w/sulfur scrubber pathways. These pathways link upstream life cycle inventory for feedstock and fuel production, with downstream use in marine engines and vessels. LCA results for these fuel pathways will be used to support the analysis performed in Maritime AGE. An overview of GREET's marine fuel pathways are provided in Table E.1.

Table E.1. Overview of GREET 2021 Marine Fuel Pathways

GREET Pathway	Feedstock(s)
HFO (2.7% sulfur)	Petroleum
HFO (0.5% sulfur)	Petroleum
HFO (0.1% sulfur)	Petroleum
MDO (1.92% sulfur)	Petroleum
MDO (0.5% sulfur)	Petroleum
MDO (0.1% sulfur)	Petroleum
MGO (1.0% sulfur)	Petroleum
MGO (0.5 % sulfur)	Petroleum
MGO (0.1 % sulfur)	Petroleum
Liquefied Natural Gas	Natural Gas
FT-Diesel	Natural Gas
FT-Diesel	Biomass & Natural Gas
FT-Diesel	Biomass & Coal
FT-Diesel	Biomass
Renewable diesel	Yellow Grease & HFO
Renewable diesel	Yellow Grease
Biodiesel	Soybean
Straight Vegetable Oil (SVO)	Soybean
Pyrolysis Oil	Woody Biomass
Methanol	Natural Gas
Methanol	Coal
Methanol	Flare Gas
Methanol	Renewable Natural Gas
Methanol	Black Liquor
Methanol	Biomass
HFO w/Scrubber	Petroleum
Ammonia (Conventional)	H_2 (from Natural Gas SMR)
Ammonia (Low Carbon)	Multiple H_2 sources[a] & N_2 sources[b]
e-Methanol	Multiple H_2 sources[c] & CO_2 from Corn Ethanol Facilities
e-FT Fuel	Multiple H_2 sources[c] & CO_2 from Corn Ethanol Facilities

[a]H_2 source(s): Byproduct H_2 from steam cracking of NGLs; H_2 from electrolysis of sodium chloride solution; H_2 from Low-temperature PEM electrolysis; H_2 from High-temperature solid oxide electrolysis

[b]N_2 Production: Cryogenic distillation or Pressure swing adsorption

[c]H_2 source(s): Solar electrolysis, Nuclear (HTGR) electrolysis, Fossil NG SMR, Nuclear (thermo cracking), Nuclear (HTG with SOEC)
SMR: Steam Methane Reforming; **FT**: Fischer-Tropsch; **H_2**: Hydrogen; **HFO**: Heavy Fuel Oil; **MDO**: Marine Distillate Oil; **MGO**: Marine Gasoil; **HTGR**: High-Temperature Gas-Cooled Reactor; **NG**: Natural Gas; **SOEC**: Solid Oxide Electrolyzer Cell

GREET's marine ammonia pathways consider both conventional ammonia (natural gas based, Haber-Bosch process), and alternative (low carbon) ammonia as a next generation maritime fuel. This effort leverages pathways originally developed for GREET in connection with the HFCTO Hydrogen@Scale and ARPA-E SmartFarm programs. The pathways have been implemented in this project for comparison and in combination with biofuels for marine use. For low carbon ammonia production, users can vary the electricity source for N_2 production and the Haber-Bosch process between the U.S. grid mix, wind electricity, and nuclear electricity. For H_2 production, users can select between low-temperature electrolysis, high temperature electrolysis, chlor-alkali process, or byproduct H_2 from stream cracking of natural gas liquids. For N_2 production, either cryogenic distillation, or pressure swing adsorption can be selected. On-going work is focused on characterizing the combustion characteristics of ammonia fuels in marine vessels, based on best available information from technical reports and peer-reviewed publications. E-methanol and e-FT fuels are modeled using CO_2 from corn ethanol plants, and two distinct system designs are considered (fuel production with or without H_2 recycle). Moreover, users can select from an array of process options such as hydrogen source (Solar electrolysis, Nuclear (HTGR) electrolysis, Fossil NG SMR, etc.), electricity source (US mix, NGCC electricity, Wind, etc.), and other key process parameters and quantify their impact on environmental performance. A HFO w/sulfur scrubber pathway was added to GREET, which includes the parasitic energy consumption for Exhaust Gas Cleaning Systems (EGCS) as well as the reduction in SOx and air-pollutant emissions during vessel operations. These new Marine pathways are available in GREET2021.

Several novel marine biofuel systems were evaluated as a next generation marine fuel including hydrothermal liquefaction (HTL) and hydrotreating of wet-wastes, landfill gas-to-diesel using Fischer-Tropsch synthesis, and bio-oil via catalytic fast pyrolysis of woody biomass. These systems are conceptually appealing in the context of marine applications due to their capacity to produce minimally processed fuels (e.g., HTL-biocrude, bio-oil, etc.). They can be blended with existing maritime fuels or further upgraded to be fungible with existing marine infrastructure and vessels. A total of 18 discrete fuel pathways were considered, an overview of the pathways including feedstock, conversion technology, and relevant metadata are provided in Table E.2.

Table E.2. FY21 Marine Biofuel Pathways evaluated To-date

ID	Feedstock	Conversion Technology	Upgrading Strategy	Final Fuel	Target or SOT	Co-Products
1	Woody Blend[1]	CFP w/ Pi/TiO2	Co-Processing[4]	Whole Oil	SOT	MEK, Acetone, Electricity
2	Woody Blend[1]	CFP w/ Pi/TiO2	Co-Processing[4]	Whole Oil	Target Case	MEK, Acetone, Electricity
3	Woody Blend[1]	CFP w/ Pi/TiO2	Co-Processing[4]	Heavy Oil	SOT	MEK, Acetone, Electricity, 'Bio-oil Light-Cut'
4	Woody Blend[1]	CFP w/ ZSM5	Co-Processing[4]	Whole Oil	SOT	MEK, Acetone, Electricity
5	Woody Blend[1]	CFP w/ ZSM5	Co-Processing[4]	Heavy Oil	SOT	MEK, Acetone, Electricity, 'Bio-oil Light-Cut'

6	Landfill Gas[2]	Fischer-Tropsch (FT)	-	FT-Diesel	-	Jet Fuel, Gasoline, Wax, Hydrogen, Electricity
7	20% Fats Oils and Greases (FOG)	HTL[3]	-	HTL-Biocrude	Target Case	-
8	Swine Manure (SM)	HTL[3]	-	HTL-Biocrude	-	-
9	Wet Waste Sludge (WWS)	HTL[3]	-	HTL-Biocrude	Target Case	-
10	Food Waste (FW)	HTL[3]	-	HTL-Biocrude	-	-
11	50% SM / 25% WWS / 20% FW / 5% FOG	HTL[3]	-	HTL-Biocrude	-	-
12	50% WWS / 40% FW / 10% FOG	HTL[3]	-	HTL-Biocrude	-	-
13	20% Fats Oils and Greases (FOG)	HTL[3]	Hydrotreating	HTL-Diesel	Target Case	Naphtha, Residue
14	Swine Manure (SM)	HTL[3]	Hydrotreating	HTL-Diesel	-	Naphtha, Residue
15	Wet Waste Sludge (WWS)	HTL[3]	Hydrotreating	HTL-Diesel	Target Case	Naphtha, Residue
16	Food Waste (FW)	HTL[3]	Hydrotreating	HTL-Diesel	-	Naphtha, Residue
17	50% SM / 25% WWS / 20% FW / 5% FOG	HTL[3]	Hydrotreating	HTL-Diesel	-	Naphtha, Residue
18	50% WWS / 40% FW / 10% FOG	HTL[3]	Hydrotreating	HTL-Diesel	-	Naphtha, Residue

[1]Woody Blend consists of 50% Clean Pine and 50% Forest Residue by mass
[2]Landfill Gas is modelled assuming a composition of 60% CH_4 and 40% CO_2 by mass
[3]Based on a 1000 Tons Per Day (TPD) refinery throughput
[4]Co-hydroprocessing of CFP oil with petroleum refinery streams is being considered as a viable means of reducing costs and enhancing commercialization potential
FOG: Fats Oils and Greases; **HTL**: Hydrothermal Liquefaction; **SM**: Swine Manure; **WWS**: Wet Waste Sludge; **FW**: Food Waste; **CFP**: Catalytic Fast Pyrolysis; **MEK**: Methyl Ester Ketone; **SOT**: State of Technology

.

References

(1) Dunn, J. B.; Newes, E.; Cai, H.; Zhang, Y.; Brooker, A.; Ou, L.; Mundt, N.; Bhatt, A.; Peterson, S.; Biddy, M. Energy, Economic, and Environmental Benefits Assessment of Co-Optimized Engines and Bio-Blendstocks. *Energy Environ. Sci.* **2020**, 10.1039.D0EE00716A. https://doi.org/10.1039/D0EE00716A.

(2) Rogers, J. N.; Stokes, B.; Dunn, J.; Cai, H.; Wu, M.; Haq, Z.; Baumes, H. An Assessment of the Potential Products and Economic and Environmental Impacts Resulting from a Billion Ton Bioeconomy. *Biofuels, Bioprod. Bioref.* **2017**, *11* (1), 110–128. https://doi.org/10.1002/bbb.1728.

(3) MEPC72, I. Resolution MEPC. 304 (72). *Initial IMO Strategy on Reduction of GHG Emissions from Ships* **2018**.